Electronic Supporting Information

From Short-bite Ligand Assembled Ribbons to Nanosized Networks in Cu(I) Coordination Polymers Built Upon Bis(benzylthio)alkanes ($BzS(CH_2)_nSBz$; n = 1-9)

Adrien Schlachter,[†] Antony Lapprand,[†,‡] Daniel Fortin,[†] Carsten Strohmann,[§]

Pierre D. Harvey,[*,†] and Michael Knorr*[*,‡]*

†Département de Chimie, Université de Sherbrooke 2550 Boulevard Université, Sherbrooke, PQ, Canada, J1K 2R1.

‡Institut UTINAM, UMR CNRS 6213, Université Bourgogne Franche-Comté, 16, Route de Gray, 25030 Besançon, France.

§Anorganische Chemie, Technische Universität Dortmund, Otto-Hahn-Straße 6, 44227 Dortmund, Germany.

Table of Contents

Experimental Section

Instrumentation

Single Crystal X-ray Structure Analyses: Single crystals of **CP1, CP10, CP12, CP15, CP16** and **CP17** were mounted on a Bruker D8 Venture four-circle diffractometer equipped with a nitrogen jet stream low-temperature system (Oxford Cryosystems). The X-ray source was graphite monochromated Mo-Kα radiation (λ = 0.71073 Å) from a microfocus sealed tube IμS by Incoatec. The lattice parameters were obtained by least-squares fit to the optimized setting angles of the entire set of collected reflections. Intensity data were recorded as ϕ and ω scans with κ offsets. No significant intensity decay or temperature drift was observed during data collections. Data were reduced by using SAINT v8.37A (Bruker, 2015) software and absorption correction was carried out by SADABS-2016/2 (Bruker, 2016). The structure was solved using SHELXT (Sheldrick, 2015) with intrinsic phasing. Refinements were carried out by full-matrix least-squares on F2 using SHELXL program (Sheldrick, 2015) on the complete set of reflections. All non–hydrogen atoms were refined with anisotropic thermal parameters, whereas the H atoms were treated in a riding mode.[1–3]

Single crystals of **CP2**, **CP3**, **CP4**, **CP5**, **CP6**, **CP7**, **CP8**, **CP9**, **CP11**, **CP13**, **CP14**, **CP18**, **CP19**, **CP20**, **CP21**, **CP22**, **CP23**, **CP24**, **CP25** and **D1** were mounted on a Bruker APEX-II DUO equipped with a nitrogen jet stream low-temperature system (Oxford Cryosystems). The X-ray source was from graphite monochromated Mo-Kα radiation (λ = 0.71073 Å) sealed tube or Cu (λ = 1.54186 Å) microfocus tube IμS with MX optics by Incoatec. The lattice parameters were obtained by least-squares fit to the optimized setting angles of the entire set of collected reflections. Intensity data were recorded as ϕ and ω scans. Data were reduced by using SAINT v8.37A (Bruker, 2015) software and absorption correction was carried out by SADABS-2016/2 (Bruker, 2016). The structure was solved using the Bruker SHELXTL Software Package. Refinement was performed with Shelxl-crystal structure refinement-multi-cpu version, G. M. Sheldrick 1993-2018 version 2018/3 on the complete set of reflections. All non–hydrogen atoms were refined with anisotropic thermal parameters.[2,3]

Powder XRD measurements: The samples for PXRD measurements were mixed with a small amount of paratone oil, cut to approximately 0.3 × 0.3 × 0.3 mm^3, and placed on a sample holder mounted at 173 K on a Bruker APEX DUO X-ray diffractometer. Six correlated runs per sample with Phi Scan of 360 degrees and exposure times of 270 s were collected with the Cu micro-

focus anode (1.54184 Å) and the CCD APEX II detector at a 150 mm distance. These runs, from −12 to −72°2θ and 6 to 36ω, were then treated and integrated with the XRW2 Eval Bruker software to produce WAXD diffraction patterns from 2.5 to 82°2θ. The patterns were treated with Diffrac.Eva version 2.0 from Bruker.

Elemental analysis: The elemental analysis (CHS) were measured on a LECO TCH600. Samples were weighed in silver caps in addition with V_2O_5. Sulfamethazine, Glycine, Benzoic Acid, Potassium Biphthalate and Stearic Acid were used as standard. The elemental analyses for **CP3**, **CP23** and **CP25** were performed by the analytical service of the University of Lorraine in Nancy, France

NMR: The ^{1}H NMR (300 MHz) spectra were recorded on a Bruker Avance 300 Ultrashield NMR spectrometer. The chemical shifts are given in ppm relative to the residual peaks of $CDCl_3$.

Thermal analysis: The thermal analysis (TGA) traces were measured on a Perkin Elmer TGA 7 apparatus in the temperature range between 25 and 950 °C at a scanning rate of 10°C.min^{-1} under argon atmosphere.

FT-Raman: The FT-Raman spectra were recorded from 0 to 4000 cm^{-1}, at 5 cm^{-1} resolution using a Bruker RFS 100/S spectrometer with the 1064 nm excitation and a light power equal to 250 mW equipped with a photomultiplier Ge-diode, cooled at liquid nitrogen temperature (77 K). The peak centred between 83 and 85 cm^{-1} is considered as residual artefact from the instrument and shouldn't be considered.

FT-IR: The IR spectra were recorded on an ABB Bomem, MB series FTIR spectrometer equipped with an ATR module from Specac from 600 to 4000 cm^{-1} with a resolution of 4 cm^{-1}.

Photophysical instrumentation: The solid-state UV-visible spectra were recorded on a Varian Cary 300 Bio UV-Vis spectrophotometer at 298 K using raised-angle transmittance apparatus and a homemade 77 K sample-holder. Samples were dispersed between two quartz plates. Solid-state emission, excitation, emission lifetimes and CIE 1931 charts (chromaticity coordinates) were acquired on a phosphorimeter FLS980 from Edinburgh Instruments equipped with single monochromators. Samples were introduced in a capillary or dispersed between two quartz plates and spectra obtained were corrected for instrument response. The emission lifetime measurements were performed using a "flash" pulsed lamp. Lifetimes values were obtained using a time correlated single photon counting (TCSPC) system and data were treated from both deconvolution of multi-exponential analysis and exponential series method. Solid state emission

quantum yields were recorded using a Quanta-φ F-3029 integration sphere from Horiba plugged into a Horiba Fluorolog III.

Synthesis

Materials. CuI, CuBr, CuCl, Benzyl mercaptan and corresponding dihalide alkane $X(CH_2)_nX$ (n = 1-9, X = I, Br) were purchased from Acros, Millipore Sigma and Oakwood Chemicals and used without further purifications. All reactions were performed using standard Schlenk techniques.

General procedure for ligands synthesis. Although the preparation of most dithioethers has already been described in the literature using different strategies such as benzyl thiol addition to allene, we have unified the experimental procedure as follows and compiled the spectroscopic data: Benzylmercaptan (2 equivalents) was deprotonated in an ethanolic solution of KOH (2.4 equivalents) in ethanol.[4] After 1h under stirring, the corresponding alkyl dihalide (1 equivalent) was added was added in several portions. Stirring continued for 1h and then the solution was refluxed for 1h. After separation of precipitated KCl (or KBr), the solvent was evaporated, the residue was washed with water and extracted with CH_2Cl_2. Recrystallisation in ethanol affords most of the ligands after storing at -20°C in form of colorless or pale yellowish crystal, which melt reaching ambient temperature to produce viscous oils.

Bis(benzylthio)methane L1. ^{1}H NMR (300 MHz, $CDCl_3$): δ (ppm): 7.32 – 7.23 (m, 10H; Ar-H), 3.84 (4H; s, CH_2), 3.39 (s, 2H; CH_2); ^{13}C NMR (101 MHz, $CDCl_3$): δ (ppm):138.26, 128.93, 128.65, 127.19, 36.39, 31.12.

1,3-bis(benzylthio)propane L2. ^{1}H NMR (300 MHz, $CDCl_3$): δ (ppm): 7.38 – 7.30 (m, 10H; Ar-H), 3.73 (s, 4H; CH_2), 2.46 (t, 4H; CH_2), 1.88 – 1.83 (t, 2H; CH_2); ^{13}C NMR (101 MHz, $CDCl_3$): δ (ppm):138.42, 128.86, 128.52, 126.99, 36.25, 30.20, 28.75.

1,4-bis(benzylthio)butane L3. ^{1}H NMR (300 MHz, $CDCl_3$): δ (ppm): 7.35 – 7.31 (m, 10H; Ar-H), 3.70 (s, 4H, CH_2), 2.40 – 2.37 (m, 4H, CH_2), 1.64 – 1.61 (m, 4H, CH_2); ^{13}C NMR (101 MHz, $CDCl_3$): δ (ppm):138.45, 128.77, 128.39, 126.84, 36.10, 30.69, 28.05.

1,6-bis(benzylthio)hexane L4. ^{1}H NMR (300 MHz, $CDCl_3$): δ (ppm): 7.3 – 7.22 (m, 10H; Ar-H), 3.60 (s, 4H; CH_2), 2.41 (t, 4H; CH_2), 1.88 – 1.79 (q, 4H; CH_2), 1.40 – 1.29 (m, 4H, CH_2); ^{13}C NMR (101 MHz, $CDCl_3$): δ (ppm):138.66, 128.85, 128.48, 126.91, 43.29, 36.34, 29.07, 28.43.

1,7-bis(benzylthio)heptane L5. ^{1}H NMR (300 MHz, $CDCl_3$): δ (ppm): 7.36 – 7.25 (m, 10H; Ar-H), 3.73 (s, 4H; CH_2), 2.43 (t, 4H, CH_2), 1.61 – 1.53 (m, 4H, CH_2), 1.41 – 1.22 (m, 6H, CH_2);

^{13}C NMR (101 MHz, $CDCl_3$): δ (ppm):138.63, 128.79, 128.40, 126.83, 36.27, 31.28, 29.09, 28.73, 28.65.

1,8-bis(benzylthio)octane L6. ^{1}H NMR (300 MHz, $CDCl_3$): δ (ppm): 7.32 – 7.21 (m, 10H; Ar-H), 3.73 (4H; CH_2), 2.42 – 2.38 (t, 4H; CH_2), 1.58 – 1.23 (m, 12H; CH_2); ^{13}C NMR (101 MHz, $CDCl_3$): δ (ppm):138.80, 128.96, 128.63, 128.59, 127.01, 36.45, 31.51, 29.31, 29.19, 28.92.

1,9-bis(benzylthio)nonane L7. ^{1}H NMR (300 MHz, $CDCl_3$): δ (ppm): 7.34 – 7.20 (m, 10H; Ar-H), 3.70 (4H; CH_2), 2.43 – 2.38 (t, 4H; CH_2), 1.59 – 1.49 (m, 4H, CH_2), 1.37– 1.23 (m, 10H; CH_2); ^{13}C NMR (101 MHz, $CDCl_3$): δ (ppm):138.75, 128.91, 128.52, 126.94, 36.40, 31.47, 29.42, 29.28, 29.22, 28.92.

General procedure for the synthesis of the CPs: All CuI-based CPs were prepared in a similar manner as previously described for the preparation of $[Cu_4I_4\{\mu\text{-}ArS(CH_2)_nSAr\}_2]_n$ and $[\{Cu(\mu_2\text{-}I)_2Cu\}\{\mu\text{-}ArS(CH_2)_nSAr\}_2]_n$ [5,6] by mixing at ambient temperature CuI with the corresponding dithioether using MeCN as solvent. To avoid formation of product mixtures, it is preferential to obtain the pure $[Cu_4I_4\{\mu\text{-}BzS(CH_2)_nSBz\}_2]_n$ compound by adding 1 equivalent of the appropriate ligand to a clear solution of two equivalents of CuI in MeCN. Partial precipitation of the white polymer occurred shortly after addition. The precipitate was the refluxed for 2-3 min until all material redissolved (sometimes by addition of an additional amount of solvent), the solution was allowed to reach slowly room temperature to yield the targeted product in crystalline form. To obtain a quasi-pure $[\{Cu(\mu_2\text{-}I)_2Cu\}\{\mu\text{-}BzS(CH_2)_nSAr\}_2]_n$ compound, solid CuI was added in several portion to MeCN solution containing an slight excess of **L**. The $[\{Cu(\mu_2\text{-}Br)_2Cu\}\{\mu\text{-}BzS(CH_2)_nSAr\}_2]_n$ compound were prepared in a similar manner. To avoid oxidation of the CuBr and CuCl containing compound to dark-green colored Cu(II) species, a mixture of deoxygenated MeCN containing ca 5% of MeOH as reducing agent was used.

Preparation of CP1. IR (ATR): 3059 (w), 3026 (w), 2959 (w), 2916 (w), 2835 (w), 2316 (w), 2168 (w), 2079 (w), 2021 (w), 1952 (w), 1879 (w), 1807 (w), 1757 (w), 1682 (w), 1601 (w), 1583 (w), 1493 (m), 1452 (m), 1427 (w), 1371 (w), 1323 (w), 1242 (w), 1200 (w), 1176 (m), 1155 (w), 1068 (m), 1028 (w), 984 (w), 918 (m), 891 (w), 864 (w), 843 (w), 768 (m), 727 (m), 708 (m), 692 (s), 619 (m) cm^{-1}; Raman: 3051 (w), 3001 (w), 2976 (w), 2957 (w), 2907 (m), 2835 (w), 1601 (m), 1582 (w), 1453 (w), 1429 (w), 1389 (w), 1240 (w), 1198 (w), 1183 (w), 1158 (w), 1131 (w), 1026 (w), 1001 (s), 803 (w), 772 (w), 726 (w), 708 (w), 675 (m), 656 (w), 618 (w), 565 (w), 477 (w), 369 (w), 338 (w), 261 (w), 213 (w), 184 (w), 137 (m), 122 (m), 99 (s) cm^{-1};

Anal. Calc for $C_{15}H_{16}CuIS_2$ (450.84): %C 39.96, %H 3.58, %S 14.22; found %C 38.91, %H 3.43, %S 14.86.

Preparation of CP2. IR (ATR): 689 (s), 766 (m), 1173 (m), 1493 (m), 1454 (m), 721 (w), 619 (w), 1068 (w), 779 (w), 860 (w), 914 (w), 1375 (w), 847 (w), 1429 (w), 1203 (w), 1246 (w), 3344 (w), 893 (w), 1028 (w), 1601 (w), 3445 (w), 1001 (w), 3026 (w), 959 (w), 1956 (w), 2914 (w), 1769 (w), 1888 (w), 2353 (w), 3061 (w), 2042 (w), 2110 (w) cm^{-1}; Anal. Calc for $C_{15}H_{16}BrCuS_2$ (403.85): %C 44.61, %H 3.99, %S 15.88; found %C 39.79, %H 3.61, %S 14.73.

Preparation of CP3. IR (ATR): 619 (m), 667 (s), 694 (s), 712 (m), 766 (m), 829 (w), 883 (w), 916 (w), 986 (w), 1026 (w), 1070 (w), 1111 (w), 1149 (w), 1175 (w), 1246 (w), 1327 (w), 1383 (w), 1421 (m), 1454 (m), 1493 (m), 1601 (w), 1693 (w), 1769 (w), 1803 (w), 1886 (w), 1952 (w), 2353 (w), 2914 (w), 2966 (w), 3030 (w), 3063 (w), 3342 (w), 3447 (w) cm^{-1}; Anal. Calc for $C_{15}H_{16}ClCuS_2$ (359.42): %C 50.13, %H 4.49, %S 17.84; found %C 49.16, %H 4.29, %S 16.99.

Preparation of CP4. IR (ATR): 619 (w), 654 (s), 671 (m), 690 (s), 756 (m), 768 (m), 804 (w), 841 (w), 879 (w), 910 (w), 999 (w), 1028 (w), 1070 (w), 1109 (w), 1140 (w), 1155 (w), 1200 (w), 1238 (w), 1265 (w), 1346 (w), 1423 (w), 1450 (m), 1491 (m), 1601 (w), 1682 (w), 1809 (w), 1886 (w), 1954 (w), 2027 (w), 2284 (w), 2908 (w), 2959 (w), 2999 (w), 3020 (w), 3078 (w) cm^{-1}; Anal. Calc for $C_{17}H_{20}CuIS_2$ (478.89): %C 42.64, %H 4.21, %S 13.39; found %C 43.20, %H 4.39, %S 12.68.

Preparation of CP5. IR (ATR): 621 (w), 656 (s), 673 (m), 694 (s), 760 (m), 768 (m), 804 (w), 849 (w), 883 (w), 910 (w), 999 (w), 1030 (w), 1072 (w), 1111 (w), 1159 (w), 1200 (w), 1238 (w), 1348 (w), 1427 (w), 1452 (m), 1493 (m), 1601 (w), 1682 (w), 1807 (w), 1888 (w), 1954 (w), 2041 (w), 2289 (w), 2905 (w), 2962 (w), 3030 (w), 3078 (w), 3418 (w), 3514 (w) cm^{-1}; Anal. Calc for $C_{17}H_{20}BrCuS_2$ (431.90): %C 47.27, %H 4.67, %S 14.85; found %C 46.19, %H 4.69, %S 12.98.

Preparation of CP6. IR (ATR): 619 (w), 654 (m), 673 (m), 698 (s), 771 (m), 806 (m), 854 (m), 914 (w), 995 (w), 1028 (w), 1072 (w), 1105 (w), 1146 (w), 1196 (w), 1236 (w), 1296 (w), 1325 (w), 1427 (w), 1445 (w), 1452 (w), 1493 (m), 1556 (w), 1601 (w), 1697 (w), 1771 (w), 1886 (w), 1954 (w), 2353 (w), 2908 (w), 2957 (w), 3003 (w), 3020 (w), 3080 (w), 3385 (w) cm^{-1}; Anal. Calc for $C_{17}H_{20}ClCuS_2$ (387.44): %C 52.70, %H 5.20, %S 16.55; found %C 41.93, %H 4.38, %S 10.98.

Preparation of CP7. IR (ATR): 619 (w), 662 (s), 696 (s), 710 (m), 721 (m), 768 (m), 802 (w), 835 (w), 893 (w), 916 (w), 966 (w), 986 (w), 1028 (w), 1068 (w), 1107 (w), 1157 (w), 1194 (w), 1238 (w), 1286 (w), 1315 (w), 1406 (m), 1416 (w), 1452 (m), 1493 (m), 1539 (w), 1583 (w), 1601 (w), 1684 (w), 1757 (w), 1801 (w), 1879 (w), 1948 (w), 1967 (w), 2905 (w), 2928 (w), 2951 (w), 3003 (w), 3024 (w) cm^{-1}; Raman: 107 (m), 199 (w), 249 (w), 282 (w), 344 (w), 402 (w), 467 (w), 571 (w), 618 (w), 677 (w), 697 (w), 712 (w), 739 (w), 768 (w), 780 (w), 816 (w), 886 (w), 988 (w), 1001 (s), 1028 (w), 1048 (w), 1065 (w), 1096 (w), 1159 (w), 1181 (w), 1200 (w), 1215 (w), 1248 (w), 1281 (w), 1296 (w), 1320 (w), 1337 (w), 1433 (w), 1455 (w), 1582 (w), 1599 (m), 2610 (w), 2708 (w), 2727 (w), 2858 (m), 2882 (m), 2909 (s), 2978 (w), 3001 (w), 3036 (m), 3051 (m), 3065 (m), 3163 (w) cm^{-1}; Anal. Calc for $C_{27}H_{33}Cu_4I_4S_3$ (1215.47): %C 26.68, %H 2.74, %S 7.91; found %C 27.56, %H 2.98, %S 7.98.

Preparation of CP8. IR (ATR): 621 (w), 654 (m), 694 (s), 770 (m), 804 (w), 851 (w), 872 (w), 889 (w), 918 (w), 1001 (w), 1028 (w), 1070 (m), 1105 (w), 1169 (w), 1202 (w), 1242 (w), 1271 (w), 1321 (w), 1418 (w), 1429 (w), 1452 (m), 1495 (m), 1583 (w), 1601 (w), 1697 (w), 1771 (w), 1888 (w), 1961 (w), 2324 (w), 2853 (w), 2922 (w), 3028 (w) cm^{-1}; Anal. Calc for $C_{36}H_{44}Cu_2I_2S_4$ (985.83): %C 43.86, %H 4.50, %S 13.01; found %C 46.72, %H 4.84, %S 13.94.

Preparation of CP9. IR (ATR): 681 (m), 704 (s), 768 (m), 775 (m), 806 (w), 849 (w), 878 (w), 920 (w), 986 (w), 1028 (w), 1070 (w), 1146 (w), 1184 (w), 1234 (w), 1277 (w), 1306 (w), 1418 (w), 1435 (w), 1452 (w), 1495 (w), 1506 (w), 1541 (w), 1558 (w), 1599 (w), 1653 (w), 1684 (w), 1697 (w), 1717 (w), 1771 (w), 2357 (w), 2930 (w) cm^{-1}; Raman: 118 (m), 143 (w), 174 (w), 220 (w), 253 (w), 288 (w), 319 (w), 344 (w), 475 (w), 508 (w), 569 (w), 619 (w), 650 (w), 662 (w), 681 (w), 704 (w), 724 (w), 745 (w), 776 (w), 807 (w), 837 (w), 876 (w), 920 (w), 976 (w), 988 (w), 1001 (s), 1009 (w), 1028 (w), 1069 (w), 1159 (w), 1177 (w), 1204 (w), 1235 (w), 1244 (w), 1306 (w), 1418 (w), 1431 (w), 1453 (w), 1495 (w), 1582 (w), 1599 (m), 1979 (w), 2058 (w), 2218 (w), 2588 (w), 2710 (w), 2845 (w), 2907 (m), 2922 (m), 2955 (w), 2968 (w), 3003 (w), 3045 (m), 3057 (m), 3159 (w), 3196 (w) cm^{-1}; Anal. Calc for $C_{18}H_{22}BrCuS_2$ (445.92): %C 48.48, %H 4.97, %S 14.38; found %C 49.37, %H 4.93, %S 14.38.

Preparation of D1. IR (ATR): 617 (w), 706 (s), 737 (w), 756 (w), 766 (w), 814 (w), 849 (w), 918 (w), 987 (w), 1028 (w), 1070 (w), 1175 (w), 1200 (w), 1230 (w), 1284 (w), 1433 (w), 1452 (s), 1495 (m), 1541 (w), 1558 (w), 1583 (w), 1601 (w), 1697 (w), 1967 (w), 2847 (w), 2928 (w), 3026 (w), 3335 (w), 3447 (w) cm^{-1}; Raman: D1 , 118 (w), 180 (w), 207 (w), 450 (w), 564 (w), 618 (w), 652 (w), 677 (w), 691 (w), 710 (w), 739 (w), 780 (w), 818 (w), 1001 (m), 1028 (w), 1156 (w), 1177 (w), 1200 (w), 1239 (w), 1250 (w), 1285 (w), 1435 (w), 1453 (w), 1495 (w),

1582 (w), 1599 (w), 1630 (w), 1823 (w), 1929 (w), 2392 (w), 2847 (w), 2922 (w), 3003 (w), 3053 (m), 3163 (w), 3352 (w), 3639 (w) cm^{-1}; Anal. Calc for $C_{36}H_{44}Cl_2Cu_2S_4$ (802.93): %C 53.85, %H 5.52, %S 15.97; found %C 53.11, %H 5.44, %S 15.52.

Preparation of CP10. IR (ATR): 619 (w), 671 (m), 698 (s), 739 (m), 770 (w), 806 (w), 849 (w), 872 (w), 918 (w), 968 (w), 986 (w), 1003 (w), 1026 (w), 1072 (w), 1113 (w), 1157 (w), 1169 (w), 1202 (w), 1238 (w), 1294 (w), 1346 (w), 1418 (w), 1431 (w), 1452 (m), 1462 (w), 1493 (w), 1556 (w), 1599 (w), 1769 (w), 1817 (w), 1886 (w), 1952 (w), 2017 (w), 2856 (w), 2914 (w), 3028 (w) cm^{-1}; Raman: 107 (s), 238 (w), 346 (w), 471 (w), 571 (w), 618 (w), 673 (m), 704 (w), 739 (w), 776 (w), 818 (w), 911 (w), 969 (w), 990 (w), 1001 (s), 1026 (w), 1073 (w), 1156 (w), 1181 (w), 1202 (w), 1240 (m), 1293 (w), 1435 (w), 1584 (w), 1599 (m), 1929 (w), 2058 (w), 2112 (w), 2187 (w), 2436 (w), 2517 (w), 2683 (w), 2855 (w), 2912 (m), 2947 (w), 3001 (w), 3047 (m), 3186 (w), 3229 (w), 3319 (w) cm^{-1}; Anal. Calc for $C_{40}H_{52}Cu_4I_4S_4$ (1422.81): %C 33.76, %H 3.68, %S 9.01; found %C 33.74, %H 4.17, %S 9.15.

Preparation of CP11. IR (ATR): 619 (w), 636 (m), 698 (s), 733 (w), 754 (w), 770 (m), 802 (w), 870 (w), 905 (w), 920 (w), 970 (w), 1001 (w), 1026 (w), 1070 (w), 1105 (w), 1148 (w), 1202 (w), 1232 (w), 1310 (w), 1360 (w), 1418 (m), 1437 (w), 1452 (m), 1462 (w), 1493 (w), 1506 (w), 1541 (w), 1558 (w), 1601 (w), 1697 (w), 1771 (w), 1944 (w), 2851 (w), 2912 (m), 2999 (w), 3022 (w), 3057 (w) cm^{-1}; Raman: 107 (s), 168 (w), 224 (w), 475 (w), 637 (w), 683 (m), 776 (w), 805 (w), 999 (s), 1026 (w), 1156 (w), 1200 (w), 1240 (m), 1298 (w), 1435 (w), 1482 (w), 1599 (m), 1831 (w), 1962 (w), 2023 (w), 2122 (w), 2147 (w), 2241 (w), 2278 (w), 2378 (w), 2428 (w), 2507 (w), 2675 (w), 2847 (w), 2916 (w), 2953 (w), 3049 (m), 3192 (w), 3911 (w) cm^{-1}; Anal. Calc for $C_{20}H_{26}CuIS_2$ (520.97): %C 46.11, %H 5.03, %S 12.31; found %C 47.00, %H 5.26, %S 12.65.

Preparation of CP12. IR (ATR): 621 (w), 640 (m), 658 (w), 700 (s), 731 (w), 771 (s), 800 (w), 829 (w), 849 (w), 868 (w), 908 (w), 922 (w), 970 (w), 1001 (w), 1028 (w), 1072 (w), 1107 (w), 1148 (w), 1175 (w), 1202 (w), 1234 (w), 1252 (w), 1310 (w), 1325 (w), 1360 (w), 1416 (m), 1435 (w), 1452 (m), 1493 (w), 1556 (w), 1583 (w), 1601 (w), 1697 (w), 1767 (w), 1817 (w), 1888 (w), 1948 (w), 2853 (w), 2916 (m), 2932 (w), 3001 (w), 3024 (w), 3051 (w) cm^{-1}; Raman: 114 (s), 132 (m), 168 (w), 272 (w), 319 (w), 434 (w), 477 (w), 567 (w), 619 (w), 639 (w), 656 (w), 689 (w), 706 (w), 778 (w), 807 (w), 847 (w), 876 (w), 988 (w), 999 (s), 1028 (w), 1042 (w), 1158 (w), 1204 (w), 1240 (w), 1252 (w), 1298 (w), 1414 (w), 1433 (w), 1582 (w), 1599 (m), 2033 (w), 2124 (w), 2394 (w), 2708 (w), 2847 (w), 2918 (m), 2953 (w), 2997 (w), 3036 (w),

3049 (m), 3198 (w), 3242 (w) cm^{-1}; Anal. Calc for $C_{20}H_{26}BrCuS_2$ (473.98): %C 50.68, %H 5.53, %S 13.53; found %C 48.65, %H 5.43, %S 13.10.

Preparation of CP13. IR (ATR): 619 (w), 640 (m), 660 (w), 700 (s), 731 (w), 771 (s), 800 (w), 829 (w), 866 (w), 908 (w), 922 (w), 970 (w), 1028 (w), 1072 (w), 1107 (w), 1148 (w), 1202 (w), 1236 (w), 1252 (w), 1311 (w), 1360 (w), 1418 (m), 1435 (w), 1454 (m), 1493 (w), 1506 (w), 1541 (w), 1558 (w), 1601 (w), 1653 (w), 1697 (w), 1717 (w), 1771 (w), 2853 (w), 2918 (m), 3001 (w), 3026 (w), 3356 (w), 3454 (w) cm^{-1}; Raman: 116 (m), 619 (w), 685 (w), 778 (w), 807 (w), 999 (s), 1200 (w), 1239 (w), 1599 (m), 1694 (w), 1771 (w), 1790 (w), 2108 (w), 2263 (w), 2372 (w), 2446 (w), 2490 (w), 2598 (w), 2696 (w), 2789 (w), 2858 (m), 2870 (w), 2918 (s), 3051 (s), 3103 (w), 3132 (w), 3190 (w), 3209 (w), 3233 (m), 3256 (w), 3323 (w), 3342 (w), 3373 (w), 3433 (w), 3483 (w), 3545 (w), 3568 (w), 3705 (w), 3782 (w), 3857 (w) cm^{-1}; Anal. Calc for $C_{20}H_{26}ClCuS_2$ (429.52): %C 55.92, %H 6.10, %S 14.93; found %C 53.38, %H 6.03, %S 13.95.

Preparation of CP14. IR (ATR): 621 (w), 636 (w), 702 (m), 725 (m), 800 (s), 835 (w), 851 (w), 881 (w), 1016 (m), 1034 (w), 1084 (w), 1103 (w), 1119 (w), 1182 (w), 1211 (w), 1275 (w), 1302 (w), 1375 (w), 1396 (w), 1425 (m), 1491 (s), 1568 (w), 1597 (w), 1651 (w), 1799 (w), 1904 (w), 1988 (w), 2015 (w), 2071 (w), 2322 (w), 2849 (w), 2922 (m), 3022 (w) cm^{-1}; Raman: 114 (m), 205 (w), 257 (w), 290 (w), 475 (w), 565 (w), 619 (w), 650 (w), 683 (w), 708 (w), 745 (w), 774 (w), 803 (w), 818 (w), 872 (w), 988 (w), 999 (m), 1028 (w), 1061 (w), 1107 (w), 1144 (w), 1156 (w), 1181 (w), 1198 (w), 1208 (w), 1239 (w), 1258 (w), 1294 (w), 1416 (w), 1429 (w), 1584 (w), 1599 (w), 2008 (w), 2513 (w), 2615 (w), 2727 (w), 2853 (w), 2887 (w), 2914 (m), 2951 (w), 2961 (w), 3001 (w), 3040 (w), 3051 (w) cm^{-1}; Anal. Calc for $C_{42}H_{56}Cu_4I_4S_4$ (1450.86): %C 34.77, %H 3.89, %S 8.84; found %C 33.5, %H 3.83, %S 8.32.

Preparation of CP15. IR (ATR): 619 (w), 654 (w), 696 (s), 737 (w), 748 (m), 771 (m), 804 (w), 833 (w), 851 (w), 872 (w), 918 (w), 957 (w), 1001 (w), 1028 (w), 1072 (m), 1153 (w), 1209 (w), 1248 (w), 1277 (w), 1292 (w), 1367 (w), 1416 (m), 1429 (m), 1452 (m), 1468 (w), 1493 (m), 1583 (w), 1599 (w), 1697 (w), 1765 (w), 1815 (w), 1888 (w), 1956 (w), 2324 (w), 2856 (w), 2922 (m), 3024 (w), 3057 (w) cm^{-1}; Anal. Calc for $C_{21}H_{28}CuIS_2$ (534.99): %C 47.14, %H 5.28, %S 11.98; found %C 46.88, % 5.08 H, %S 11;68.

Preparation of CP16. IR (ATR): 621 (w), 654 (w), 696 (s), 710 (s), 739 (m), 748 (m), 773 (m), 835 (w), 851 (w), 874 (w), 918 (w), 957 (w), 1001 (w), 1026 (w), 1074 (w), 1153 (w), 1176 (w), 1207 (w), 1246 (w), 1277 (w), 1292 (w), 1325 (w), 1418 (m), 1431 (m), 1450 (m), 1470 (w), 1493 (w), 1583 (w), 1599 (w), 1763 (w), 1813 (w), 1888 (w), 1954 (w), 2048 (w), 2152 (w),

2164 (w), 2334 (w), 2856 (w), 2922 (m), 3028 (w), 3055 (w) cm^{-1}; Raman: 112 (s), 159 (w), 205 (w), 261 (w), 290 (w), 321 (w), 477 (w), 502 (w), 565 (w), 619 (w), 652 (m), 685 (w), 708 (w), 747 (w), 772 (w), 803 (w), 874 (w), 988 (w), 999 (s), 1028 (w), 1063 (w), 1142 (w), 1156 (w), 1163 (w), 1175 (w), 1196 (w), 1206 (w), 1239 (m), 1246 (w), 1294 (w), 1418 (w), 1429 (w), 1582 (w), 1599 (m), 2120 (w), 2172 (w), 2446 (w), 2583 (w), 2725 (w), 2853 (w), 2887 (m), 2916 (m), 2943 (w), 2957 (w), 2976 (w), 3001 (w), 3026 (w), 3040 (w), 3055 (m) cm^{-1}; Anal. Calc for $C_{21}H_{28}BrCuS_2$ (488.00): %C 51.68, %H 5.78, %S 13.14; found %C 53.43, %H 5.90, %S 13.09.

Preparation of CP17. IR (ATR): 656 (w), 698 (s), 710 (s), 748 (m), 771 (m), 851 (w), 874 (w), 918 (w), 957 (w), 1001 (w), 1028 (w), 1074 (w), 1151 (w), 1207 (w), 1246 (w), 1277 (w), 1292 (w), 1418 (m), 1431 (w), 1450 (m), 1470 (w), 1493 (w), 1583 (w), 1599 (w), 1765 (w), 1888 (w), 1954 (w), 1994 (w), 2052 (w), 2152 (w), 2332 (w), 2858 (w), 2922 (m), 3028 (w), 3055 (w), 3344 (w) cm^{-1}; Raman: 112 (s), 159 (w), 205 (w), 261 (w), 290 (w), 321 (w), 477 (w), 502 (w), 565 (w), 619 (w), 652 (m), 685 (w), 708 (w), 747 (w), 772 (w), 803 (w), 874 (w), 988 (w), 999 (s), 1028 (w), 1063 (w), 1142 (w), 1156 (w), 1163 (w), 1175 (w), 1196 (w), 1206 (w), 1239 (m), 1246 (w), 1294 (w), 1418 (w), 1429 (w), 1582 (w), 1599 (m), 2120 (w), 2172 (w), 2446 (w), 2583 (w), 2725 (w), 2853 (w), 2887 (m), 2916 (m), 2943 (w), 2957 (w), 2976 (w), 3001 (w), 3026 (w), 3040 (w), 3055 (m) cm^{-1}; Anal. Calc for $C_{21}H_{28}ClCuS_2$ (443.54): %C 56.86, %H 6.36, %S 14.46; found %C 60.14, %H 6.70, %S 15.36.

Preparation of CP18. IR (ATR): 631 (w), 698 (s), 721 (w), 748 (w), 771 (m), 806 (w), 883 (w), 1026 (w), 1072 (w), 1144 (w), 1200 (w), 1213 (w), 1234 (w), 1296 (w), 1416 (m), 1429 (w), 1452 (m), 1462 (w), 1493 (w), 1556 (w), 1583 (w), 1601 (w), 1651 (w), 1771 (w), 1979 (w), 2851 (m), 2922 (m), 3026 (w), 3626 (w) cm^{-1}; Anal. Calc for $C_{44}H_{60}Cu_4I_4S_4$ (1478.92): %C 35.73, %H 4.09, %S 8.67; found %C 38.53, %H 4.60, %S 9.69.

Preparation of CP19. IR (ATR): 633 (w), 698 (s), 721 (w), 731 (w), 748 (w), 771 (m), 806 (w), 824 (w), 885 (w), 897 (w), 966 (w), 984 (w), 1028 (w), 1072 (w), 1144 (w), 1159 (w), 1202 (w), 1213 (w), 1234 (w), 1281 (w), 1296 (w), 1325 (w), 1356 (w), 1414 (m), 1429 (w), 1454 (m), 1464 (w), 1495 (w), 1556 (w), 1583 (w), 1601 (w), 1697 (w), 1759 (w), 1809 (w), 1879 (w), 1956 (w), 2353 (w), 2851 (m), 2922 (m), 3028 (w) cm^{-1}; Raman: 107 (s), 130 (w), 220 (w), 265 (w), 282 (w), 351 (w), 631 (w), 672 (w), 801 (w), 832 (s), 849 (w), 905 (w), 980 (w), 1125 (w), 1181 (w), 1291 (w), 1320 (w), 1408 (w), 1451 (w), 1576 (w), 1630 (s), 1807 (w), 2276 (w), 2623 (w), 2804 (w), 3009 (w), 3074 (w), 3086 (m), 3219 (w) cm^{-1}; Anal. Calc for $C_{22}H_{30}CuIS_2$ (549.02): %C 48.13, %H 5.51, %S 11.68; found %C 50.50, %H 5.88, %S 11.85.

Preparation of CP20.

IR (ATR): 474 (m), 567 (m), 702 (s), 745 (w), 773 (m), 849 (w), 873 (w), 1027 (w), 1073 (w), 1147 (w), 1205 (w), 1243 (w), 1277 (w), 1417 (w), 1451 (w), 1493 (w), 1599 (w), 2855 (w), 2920 (m), 3028 (w), 3339 (w), 3444 (w) cm^{-1}; Anal. Calc for $C_{44}H_{60}Br_2Cu_2S_4$ (1004.06): %C 52.63, %H 6.02, %S 12.77; found %C 52.93, %H 5.78, %S 12.41.

Preparation of CP21. IR (ATR): 619 (w), 675 (m), 694 (s), 717 (w), 731 (w), 744 (w), 766 (m), 839 (w), 883 (w), 914 (w), 982 (m), 1022 (s), 1078 (m), 1180 (w), 1229 (w), 1292 (w), 1416 (w), 1454 (m), 1472 (m), 1495 (m), 1541 (w), 1558 (w), 1603 (w), 1682 (w), 1809 (w), 1896 (w), 2041 (w), 2845 (m), 2918 (m), 2959 (w), 3034 (w), 3063 (w), 3340 (w), 3445 (w) cm^{-1}; Anal. Calc for $C_{44}H_{60}Cl_2Cu_2S_4$ (915.14): %C 57.75, %H 6.61, %S 14.01; found %C 60.84, %H 7.19, %S 15.70.

Preparation of CP22. IR (ATR): 698 (s), 721 (w), 770 (m), 808 (w), 874 (w), 916 (w), 1028 (w), 1070 (w), 1215 (w), 1240 (w), 1418 (w), 1452 (w), 1493 (w), 1506 (w), 1520 (w), 1541 (w), 1558 (w), 1601 (w), 1636 (w), 1653 (w), 1684 (w), 1697 (w), 1717 (w), 1749 (w), 1771 (w), 1867 (w), 2041 (w), 2177 (w), 2353 (w), 2849 (w), 2924 (m), 3024 (w) cm^{-1}; Raman: 118 (m), 187 (w), 340 (w), 400 (w), 471 (w), 569 (w), 619 (w), 679 (w), 739 (w), 772 (w), 816 (w), 872 (w), 988 (w), 1001 (m), 1026 (w), 1071 (w), 1096 (w), 1158 (w), 1183 (w), 1202 (w), 1240 (w), 1294 (w), 1429 (w), 1453 (w), 1495 (w), 1584 (w), 1601 (w), 2043 (w), 2444 (w), 2610 (w), 2679 (w), 2712 (w), 2847 (w), 2885 (w), 2914 (m), 2974 (w), 3001 (w), 3038 (w), 3051 (w), 3206 (w) cm^{-1}; Anal. Calc for $C_{92}H_{128}Cu_8I_8S_8$ (3013.94): %C 36.66, %H 4.28, %S 8.51; found %C 37.18, %H 4.56, %S 8.32.

Preparation of CP23. IR (ATR): 619 (w), 696 (s), 768 (m), 810 (w), 872 (w), 914 (w), 1028 (w), 1070 (w), 1155 (w), 1238 (w), 1418 (w), 1452 (m), 1493 (m), 1506 (w), 1522 (w), 1541 (w), 1558 (w), 1601 (w), 1636 (w), 1653 (w), 1684 (w), 1697 (w), 1717 (w), 1749 (w), 1792 (w), 1942 (w), 2851 (w), 2922 (m), 3026 (w) cm^{-1}; Raman: 107 (m), 199 (w), 249 (w), 282 (w), 344 (w), 402 (w), 467 (w), 571 (w), 618 (w), 677 (w), 697 (w), 712 (w), 739 (w), 768 (w), 780 (w), 816 (w), 886 (w), 988 (w), 1001 (s), 1028 (w), 1048 (w), 1065 (w), 1096 (w), 1159 (w), 1181 (w), 1200 (w), 1215 (w), 1248 (w), 1281 (w), 1296 (w), 1320 (w), 1337 (w), 1433 (w), 1455 (w), 1582 (w), 1599 (w), 2610 (w), 2708 (w), 2727 (w), 2858 (w), 2882 (m), 2909 (m), 2978 (w), 3001 (w), 3036 (w), 3051 (m), 3065 (w), 3163 (w) cm^{-1}; Anal. Calc for $C_{23}H_{32}CuIS_2$ (563.04): %C 49.06, %H 5.73, %S 11.39; found %C 48.99, %H 5.60, %S 11.17.

Preparation of CP24. IR (ATR): 617 (w), 698 (s), 714 (s), 729 (m), 762 (w), 843 (w), 870 (w), 920 (w), 1030 (w), 1072 (w), 1155 (w), 1215 (w), 1236 (w), 1308 (w), 1338 (w), 1418 (w), 1454 (m), 1470 (w), 1493 (m), 1506 (w), 1522 (w), 1541 (w), 1558 (w), 1601 (w), 1636 (w), 1653 (w), 1684 (w), 1697 (w), 1717 (w), 1749 (w), 2858 (m), 2922 (m), 3028 (w) cm^{-1}; Raman: 118 (w), 278 (w), 349 (w), 405 (w), 463 (w), 618 (w), 681 (w), 699 (w), 716 (w), 743 (w), 762 (w), 780 (w), 816 (w), 988 (w), 1001 (m), 1028 (w), 1048 (w), 1094 (w), 1163 (w), 1181 (w), 1200 (w), 1246 (w), 1298 (w), 1437 (w), 1582 (w), 1599 (w), 1798 (w), 2058 (w), 2216 (w), 2423 (w), 2615 (w), 2727 (w), 2856 (w), 2882 (m), 2907 (m), 2943 (w), 2953 (w), 2976 (w), 3001 (w), 3036 (w), 3051 (m), 3065 (w), 3466 (w) cm^{-1}; Anal. Calc for $C_{23}H_{32}BrCuS_2$ (516.05): %C 53.53, %H 6.25, %S 12.42; found %C 52.69, %H 6.21, %S 11.58.

Preparation of CP25. IR (ATR): 698 (s), 716 (m), 729 (m), 762 (w), 849 (w), 922 (m), 943 (m), 1020 (m), 1072 (w), 1153 (w), 1203 (w), 1236 (w), 1310 (w), 1416 (w), 1454 (m), 1470 (m), 1493 (m), 1541 (w), 1601 (w), 1697 (w), 2851 (m), 2922 (m), 3030 (w), 3063 (w), 3337 (w), 3445 (w), 3647 (w), 3749 (w), 3852 (w) cm^{-1}; Raman: 118 (w), 494 (w), 618 (w), 683 (w), 745 (w), 859 (w), 1001 (w), 1030 (w), 1094 (w), 1200 (w), 1250 (w), 1364 (w), 1439 (w), 1580 (w), 1599 (w), 1721 (w), 1778 (w), 1867 (w), 1912 (w), 1939 (w), 2021 (w), 2156 (w), 2183 (w), 2284 (w), 2371 (w), 2419 (w), 2486 (w), 2606 (w), 2729 (w), 2858 (w), 2882 (w), 2905 (w), 3001 (w), 3036 (w), 3051 (w), 3098 (w), 3277 (w), 3356 (w), 3396 (w), 3454 (w), 3553 (w) cm^{-1}; Anal. Calc for $C_{23}H_{32}ClCuS_2$ (471.59): %C 58.57, %H 6.84, %S 13.60; found %C 58.18, %H 6.70, %S 13.31.

Crystal Structures and data

Table S1. Crystal data, data collection, and structure refinement for **CP1-6**.

Compound	**CP1**	**CP2**	**CP3**	**CP4**	**CP5**	**CP6**
Formula	$C_{15}H_{16}CuIS_2$	$C_{15}H_{16}BrCuS_2$	$C_{15}H_{16}ClCuS_2$	$C_{17}H_{20}CuIS_2$	$C_{17}H_{20}BrCuS_2$	$C_{17}H_{20}S_2ClCu$
Formula weight	450.84	403.85	359.39	478.89	431.90	387.44
Temperature/K	99.99	173(2)	173(2)	173(2)	173(2)	173(2)
Wavelength/Å	0.71073	0.71073	1.54184	0.71073	1.54178	1.54178
Crystal system	triclinic	monoclinic	orthorhombic	monoclinic	monoclinic	monoclinic
Space group	*P*-1	*P* 1 2_1/*n* 1	7.0892(3)	*P* 1 2_1/*c* 1	*P* 1 2_1 1	*P* 2_1
a/Å	6.5528(7)	6.5978(2)	12.6546(5)	12.6329(10)	11.2623(4)	10.9752(4)
b/Å	9.0715(15)	13.7772(4)	33.7012(12)	6.5214(5)	6.0104(2)	5.9477(2)
c/Å	28.354(3)	17.9010(6)	7.0892(3)	21.9596(15)	12.6357(5)	12.9310(4)
α/°	90.484(6)	90	90	90	90	90
β/°	94.200(4)	91.3470(10)	90	96.802(2)	96.3270(10)	95.8400(10)
γ/°	100.821(6)	90	90	90	90	90
Volume/ $Å^3$	1650.6(4)	1626.74(9)	3023.4(2)	1796.4(2)	850.11(5)	839.72(5)
Z	4	4	8	4	2	2
Density (calc.) g/cm^3	1.814	1.649	1.579	1.771	1.687	1.532
Absorption coefficient/mm^{-1}	3.431	4.039	6.088	3.158	6.764	5.524
F(000)	880.0	808	1472	944	436	400
Crystal size/mm	0.425 × 0.099 × 0.053	0.150 × 0.200 × 0.520	0.050 × 0.205 × 0.245	0.100 × 0.210 × 0.365	0.050 × 0.165 × 0.250	0.45 × 0.19 × 0.085
2θ range for data collection/°	4.322 to 55.994	3.74 to 53.42	26.44 to 141.92	3.24 to 52.82	7.90 to 141.46	6.872 to 142.308
Index ranges	$-8 \le h \le 7$, $-11 \le k \le 11$, $-37 \le l \le 37$	$-8 \le h \le 8$, $-17 \le k \le 17$, $-22 \le l \le 22$	$-7 \le h \le 8$, $-15 \le k \le 13$, $-41 \le l \le 40$	$-15 \le h \le 15$, $-8 \le k \le 8$, $-27 \le l \le 26$	$-13 \le h \le 13$, $-6 \le k \le 7$, $-15 \le l \le 14$	$-13 \le h \le 12$, $-7 \le k \le 6$, $-15 \le l \le 15$
Reflections collected	30717	23283	32214	23062	10940	9280
Independent reflections	7894 [*R*(int) = 0.0301]	3437 [*R*(int) = 0.0273]	2706 [*R*(int) = 0.0829]	3668 [*R*(int) = 0.0531]	2940 [R(int) = 0.0417]	2853 [R(int) = 0.0706]
Refinement method	Full-matrix least-squares on F^2	Full-matrix least-squares on F^2	Full-matrix least-squares on F^2	Full-matrix least-squares on F^2	Full-matrix least-squares on F^2	Full-matrix least-squares on F^2
Data / restraints / parameters	7894/0/344	3437/0/160	2706/0/172	3668/0/190	2940/1/190	2853/1/191
Goodness-of-fit on F^2	1.045	1.033	1.071	1.045	1.120	1.090
Final *R* indices [$I > 2\sigma(I)$]	$R_1 = 0.0236$, $wR_2 = 0.0418$	$R_1 = 0.0298$, $wR_2 = 0.0698$	$R_1 = 0.0719$, $wR_2 = 0.1788$	$R_1 = 0.0772$, $wR_2 = 0.1962$	$R_1 = 0.0263$, $wR_2 = 0.0653$	$R_1 = 0.0573$, $wR_2 = 0.1566$
R indices (all data)	$R_1 = 0.0332$, $wR_2 = 0.0436$	$R_1 = 0.0375$, $wR_2 = 0.0736$	$R_1 = 0.0829$, $wR_2 = 0.1922$	$R_1 = 0.0879$, $wR_2 = 0.2012$	$R_1 = 0.0270$, $wR_2 = 0.0656$	$R_1 = 0.0628$, $wR_2 = 0.1660$
Largest diff. peak and hole/e. $Å^{-3}$	1.16 and -0.88	1.641 and -0.150	1.043 and -0.781	2.631and -1.729	0.460 and -0.461	0.98 and -0.60

Table S2. Crystal data, data collection, and structure refinement for **D1** and **CP7-11**.

Compound	**CP7**	**CP8**	**CP9**	**D1**	**CP10**	**CP11**
Formula	$C_{27}H_{33}Cu_4I_4S_3$	$C_{36}H_{44}Cu_2I_2S_4$	$C_{18}H_{22}BrCuS_2$	$C_{36}H_{44}Cl_2Cu_2S_4$	$C_{40}H_{52}Cu_4I_4S_4$	$C_{20}H_{26}CuIS_2$
Formula weight	1215.47	985.83	445.92	802.93	1422.81	520.97
Temperature/K	173(2)	173(2)	173(2)	173(2)	100	173(2)
Wavelength/Å	0.71073	0.71073	0.71073	0.71073	0.71073	0.71073
Crystal system	trigonal	triclinic	triclinic	monoclinic	orthorhombic	triclinic
Space group	*P* -3	*P* -1	*P* -1	*P* 1 2_1/*n* 1	*P* 2_1 2_1 2_1	*P* -1
a/Å	16.8558(15)	10.138(3)	9.7482(9)	13.269(3)	13.7995(15)	7.7825(12)
b/Å	16.8558(15)	10.492(3)	10.9648(10)	9.553(2)	13.7966(14)	11.5069(19)
c/Å	7.0149(6)	10.834(3)	19.3140(17)	15.333(3)	24.793(3)	12.706(2)
α/°	90	106.165(2)	86.9430(10)	90	90	103.164(7)
β/°	90	104.110(2)	83.1160(10)	109.865(2)	90	96.937(6)
γ/°	120	104.837(2)	66.2700(10)	90	90	103.594(6)
Volume/ $Å^3$	1726.0(3)	1006.4(4)	1876.2(3)	1827.9(7)	4720.3(9)	1058.5(3)
Z	2	1	4	2	4	2
Density (calc.) g/cm^3	2.339	1.627	1.579	1.459	2.002	1.635
Absorption coefficient/mm^{-1}	6.207	2.821	3.510	1.563	4.598	2.687
F(000)	1142	488	904	832	2736	520
Crystal size/mm	0.230 × 0.300 × 0.300	0.135 × 0.215 × 0.435	0.250 × 0.295 × 0.300	0.075 × 0.250 × 0.370	0.307 × 0.204 × 0.203	0.100 × 0.140 × 0.306
2*θ* range for data collection/°	5.58 to 52.84	4.16 to 52.82	2.12 to 52.82	3.52 to 52.82	4.174 to 63.984	3.36 to 52.94
Index ranges	$-21 \le h \le 21$, $-21 \le k \le 21$, $-8 \le l \le 8$	$-12 \le h \le 12$, $-13 \le k \le 13$, $-13 \le l \le 13$	$-12 \le h \le 12$, $-13 \le k \le 13$, $-23 \le l \le 24$	$-16 \le h \le 16$, $-11 \le k \le 11$, $-19 \le l \le 19$	$-20 \le h \le 20$, $-20 \le k \le 20$, $-36 \le l \le 36$	$-9 \le h \le 9$, $-14 \le k \le 14$, $-15 \le l \le 15$
Reflections collected	24912	14316	27328	25397	279363	14562
Independent reflections	2369 [*R*(int) = 0.0161]	4117 [*R*(int) = 0.0197]	7671 [*R*(int) = 0.0173]	3744 [*R*(int) = 0.0515]	16363 [*R*(int) = 0.0522]	4339 [*R*(int) = 0.1009]
Refinement method	Full-matrix least-squares on F^2	Full-matrix least-squares on F^2	Full-matrix least-squares on F^2	Full-matrix least-squares on F^2	Full-matrix least-squares on F^2	Full-matrix least-squares on F^2
Data / restraints / parameters	2369/0/115	4117/0/185	7671 / 0 / 385	3744/0/199	16363/0/470	4339/0/217
Goodness-of-fit on F^2	1.263	1.141	1.030	1.088	1.052	1.032
Final *R* indices [$I > 2\sigma(I)$]	$R_1 = 0.0130$, $wR_2 = 0.0300$	$R_1 = 0.0678$, $wR_2 = 0.1617$	$R_1 = 0.0242$, $wR_2 = 0.0518$	$R_1 = 0.0406$, $wR_2 = 0.1080$	$R_1 = 0.0233$, $wR_2 = 0.0580$	*$R_1 = 0.0858$, $wR_2 = 0.2172$*
R indices (all data)	$R_1 = 0.0136$, $wR_2 = 0.0302$	$R_1 = 0.0846$, $wR_2 = 0.1745$	$R_1 = 0.0303$, $wR_2 = 0.0539$	$R_1 = 0.0490$, $wR_2 = 0.1140$	$R_1 = 0.0238$, $wR_2 = 0.0586$	*$R_1 = 0.1248$, $wR_2 = 0.2570$*
Largest diff. peak and hole/e. $Å^{-3}$	0.350 and -0.511	1.829 and -2.778	0.800 and -0.863	0.990 and -0.505	2.20 and -1.31	3.116 and -2.582

Table S3. Crystal data, data collection, and structure refinement for **CP12-17**.

Compound	**CP12**	**CP13**	**CP14**	**CP15**	**CP16**	**CP17**
Formula	$C_{20}H_{26}BrCuS_2$	$C_{20}H_{26}ClCuS_2$	$C_{42}H_{56}Cu_4I_4S_4$	$C_{21}H_{28}CuIS_2$	$C_{21}H_{28}BrCuS_2$	$C_{21}H_{28}ClCuS_2$
Formula weight	473.98	429.52	1450.86	534.99	488	443.54
Temperature/K	100	173(2)	173(2)	100	100	100
Wavelength/Å	0.71073	0.71073	0.71073	0.71073	0.71073	0.71073
Crystal system	triclinic	triclinic	monoclinic	orthorhombic	orthorhombic	orthorhombic
Space group	*P* -1	*P* -1	*C* 1 *c* 1	*P b c a*	*P b c a*	*P b c a*
a/Å	7.3967(4)	7.4239(5)	20.54(4)	10.9200(10)	10.8389(5)	10.8855(5)
b/Å	11.8505(5)	11.7060(7)	20.53(3)	17.4804(13)	17.0802(8)	16.9611(9)
c/Å	12.2279(6)	12.3199(9)	15.83(3)	23.407(2)	23.2094(11)	23.1275(9)
α/°	72.773(3)	71.455(2)	90	90	90	90
β/°	75.012(3)	74.921(3)	130.42(2)	90	90	90
γ/°	89.471(3)	88.160(2)	90	90	90	90
Volume/ Å^3	986.28(9)	978.61(11)	5082.(15)	4468.1(7)	4296.8(3)	4270.0(3)
Z	2	2	4	8	8	8
Density (calc.) g/cm^3	1.596	1.458	1.896	1.591	1.509	1.380
Absorption coefficient/mm^{-1}	3.344	1.465	4.272	2.548	3.073	1.345
F(000)	484	448	2800	2144	2000	1856
Crystal size/mm	0.70 × 0.38 × 0.29	0.190 × 0.230 × 0.270	0.160 × 0,165 × 0.245	0.268 × 0.150 × 0.080	0.783 × 0.166 × 0.144	0.286 × 0.122 × 0.057
2θ range for data collection/°	6.534 to 69.994	3.62 to 52.82	3.28 to 52.86	4.974 to 63.318	5.082 to 61.196	5.166 to 60.964
Index ranges	$-11 \le h \le 11$, $-19 \le k \le 19$, $-19 \le l \le 19$	$-9 \le h \le 9$, $-14 \le k \le 14$, $-15 \le l \le 15$	$-23 \le h \le 25$, $-25 \le k \le 25$, $-19 \le l \le 19$	$0 \le h \le 15$, $0 \le k \le 20$, $0 \le l \le 34$	$-15 \le h \le 10$, $-22 \le k \le 24$, $-32 \le l \le 32$	$-15 \le h \le 15$, $-24 \le k \le 123$, $-33 \le l \le 31$
Reflections collected	44313	14083	24484	7043	30397	197622
Independent reflections	8662 [*R*(int) = 0.0448]	3966 [*R*(int) = 0.0655]	9632 [*R*(int) = 0.1252]	7043 [*R*(int) = 0.0494]	6554 [*R*(int) = 0.0387]	6288 [*R*(int) = 0.0672]
Refinement method	Full-matrix least-squares on F^2	Full-matrix least-squares on F^2	Full-matrix least-squares on F^2	Full-matrix least-squares on F^2	Full-matrix least-squares on F^2	Full-matrix least-squares on F^2
Data / restraints / parameters	8662/0/217	3966/0/217	9632/16/486	7043/0/226	6554/0/226	3692/0/226
Goodness-of-fit on F^2	1.032	1.005	1.016	1.056	1.023	1.075
Final *R* indices [$I > 2\sigma(I)$]	$R_1 = 0.0225$, $wR_2 = 0.0561$	$R_1 = 0.0560$, $wR_2 = 0.1359$	$R_1 = 0.0855$, $wR_2 = 0.1532$	$R_1 = 0.0322$, $wR_2 = 0.0648$	$R_1 = 0.0270$, $wR_2 = 0.0543$	$R_1 = 0.0369$, $wR_2 = 0.630$
R indices (all data)	$R_1 = 0.0262$, $wR_2 = 0.0578$	$R_1 = 0.0974$, $wR_2 = 0.1574$	$R_1 = 0.2199$, $wR_2 = 0.1993$	$R_1 = 0.0415$, $wR_2 = 0.0674$	$R_1 = 0.0438$, $wR_2 = 0.0592$	$R_1 = 0.10614$, $wR_2 = 0.0676$
Largest diff. peak and hole/e. Å^{-3}	0.941 and -0.577	0.522 and -0.477	0.951 and -0.614	1.94 and -1.06	0.80 and -0.58	0.74 and -0.676

Table S4. Crystal data, data collection, and structure refinement for **CP18-22**.

Compound	**CP18**	**CP19**	**CP20**	**CP21**	**CP22**	**CP22**
Formula	$C_{44}H_{60}Cu_4I_4S_4$	$C_{22}H_{30}CuIS_2$	$C_{44}H_{60}Br_2Cu_2S_4$	$C_{44}H_{60}Cl_2Cu_2S_4$	$C_{46}H_{64}Cu_4I_4S_4$	$C_{92}H_{128}Cu_8I_8S_8$
Formula weight	1478.92	549.02	1004.06	915.14	1506.97	3013.94
Temperature/K	173(2)	173(2)	173(2)	173(2)	100(2)	173(2)
Wavelength/Å	0.71073	0.71073	0.71073	0.71073	0.71073	0.71073
Crystal system	tetragonal	monoclinic	monoclinic	monoclinic	orthorhombic	monoclinic
Space group	*I* -4 2 *d*	*P* 1 2_1 / *c* 1	*P* 1 2_1 / *c* 1	*P* 1 2_1 / *c* 1	*P b c a*	*P* 1 2_1 / *c* 1
a/Å	14.3941(18)	11.9524(7)	12.285(2)	12.2760(9)	18.0251(11)	16.0105(18)
b/Å	14.3940	9.8143(6)	12.861(2)	12.7825(9)	15.7777(9)	38.827(4)
c/Å	24.513(3)	20.2110(13)	28.987(5)	28.679(2)	38.507(2)	17.6923(17)
α/°	90	90	90	90	90	90
β/°	90	102.7150(10)	94.596(5)	93.965(2)	90	91.062(4)
γ/°	90	90	90	90	90	90
Volume/ $Å^3$	5078.8(9)	2312.7(2)	4565.1(15)	4489.5(6)	10951.2(11)	10996.3(19)
Z	4	4	4	4	8	4
Density (calc.) g/cm^3	1.934	1.577	1.461	1.354	1.828	1.820
Absorption coefficient/mm^{-1}	4.277	2.464	2.894	1.282	3.969	3.953
F(000)	2864	1104	2064	1920	5856	5856
Crystal size/mm	0.19 × 0.20 × 0.27	0.120 × 0.250 × 0.375	0.10 × 0.12 × 0.61	0.09 × 0.10 × 0.23	0.060 × 0.220 × 0.320	0.110 × 0.184 × 0.190
2θ range for data collection/°	3.28 to 52.98	3.50 to 52.76	3.32 to 54.14	2.84 to 52.96	3.10 to 52.76	2.10 to 53.22
Index ranges	$-18 \le h \le 11$, $-18 \le k \le 18$, $-30 \le l \le 27$	$-14 \le h \le 14$, $-12 \le k \le 12$, $-25 \le l \le 25$	$-15 \le h \le 15$, $-16 \le k \le 16$, $-35 \le l \le 36$	$-13 \le h \le 15$, $-16 \le k \le 16$, $-25 \le l \le 35$	$-22 \le h \le 22$, $-19 \le k \le 19$, $-48 \le l \le 47$	$-19 \le h \le 20$, $-48 \le k \le 48$, $-22 \le l \le 21$
Reflections collected	13561	32496	16322	24310	123623	114361
Independent reflections	2623 [*R*(int) = 0.0286]	4729 [*R*(int) = 0.0229]	9542 [*R*(int) = 0.0707]	9251[*R*(int) = 0.0933]	11092 [*R*(int) = 0.1365]	21001 [*R*(int) = 0.1730]
Refinement method	Full-matrix least-squares on F^2	Full-matrix least-squares on F^2	Full-matrix least-squares on F^2	Full-matrix least-squares on F^2	Full-matrix least-squares on F^2	Full-matrix least-squares on F^2
Data / restraints / parameters	2623/0/127	4729/0/235	9542/0/469	9251/4/409	11092/1/416	21001/0/751
Goodness-of-fit on F^2	1.054	1.041	1.004	1.135	1.094	1.061
Final *R* indices [$I > 2\sigma(I)$]	$R_1 = 0.0397$, $wR_2 = 0.1043$	$R_1 = 0.0211$, $wR_2 = 0.0509$	$R_1 = 0.0813$, $wR_2 = 0.1783$	$R_1 = 0.0697$, $wR_2 = 0.1465$	$R_1 = 0.0762$, $wR_2 = 0.1483$	$R_1 = 0.1313$, $wR_2 = 0.2692$
R indices (all data)	$R_1 = 0.0430$, $wR_2 = 0.1071$	$R_1 = 0.0259$, $wR_2 = 0.0531$	$R_1 = 0.1817$, $wR_2 = 0.2150$	$R_1 = 0.1443$, $wR_2 = 0.1632$	$R_1 = 0.1195$ $wR_2 = 0.1642$	$R_1 = 0.2254$, $wR_2 = 0.3087$
Largest diff. peak and hole/e. $Å^{-3}$	3.376 and -0.423	0.488 and -0.456	1.853 and -1.038	1.305 and -2.089	2.098 and -1.398	2.337 and -1.993

Table S5. Crystal data, data collection, and structure refinement for **CP23-25**.

Compound	**CP23**	**CP24**	**CP25**
Formula	$C_{23}H_{32}CuIS_2$	$C_{23}H_{32}BrCuS_2$	$C_{23}H_{32}ClCuS_2$
Formula weight	563.04	516.05	471.59
Temperature/K	173(2)	173(2)	173(2)
Wavelength/Å	0.71073	0.71073	0.71073
Crystal system	triclinic	triclinic	triclinic
Space group	*P* -1	*P* -1	*P* -1
a/Å	10.0146(15)	10.2310(16)	10.110(3)
b/Å	11.1185(16)	10.6498(16)	10.550(3)
c/Å	12.0876(18)	11.9697(18)	11.809(3)
α/°	89.5690(10)	90.3340(10)	90.569(3)
β/°	67.8700(10)	112.5540(10)	112.726(3)
γ/°	81.7520(10)	99.7910(10)	99.878(3)
Volume/ Å^3	1232.3(3)	1183.3(3)	1140.5(6)
Z	2	2	2
Density (calc.) g/cm^3	1.517	1.448	1.373
Absorption coefficient/mm^{-1}	2.314	2.794	1.264
F(000)	558	532	496
Crystal size/mm	0.200 × 0.240 × 0.450	0.080 × 0.205 × 0.425	0.100 × 0.220 × 0.260
2θ range for data collection/°	4.58 to 53.00	3.70 to 51.38	3.76 to 52.78
Index ranges	$-12 \le h \le 12$, $-13 \le k \le 13$, $-15 \le l \le 15$	$-12 \le h \le 12$, $-12 \le k \le 12$, $-14 \le l \le 14$	$-12 \le h \le 12$, $-13 \le k \le 13$, $-14 \le l \le 14$
Reflections collected	17776	16432	16635
Independent reflections	5033 [*R*(int) = 0.0213]	4490 [*R*(int) = 0.0196]	4658 [*R*(int) = 0.0719]
Refinement method	Full-matrix least-squares on F^2	Full-matrix least-squares on F^2	Full-matrix least-squares on F^2
Data / restraints / parameters	5033 /0 / 238	4490 / 0 / 226	4658 / 0 / 244
Goodness-of-fit on F^2	1.158	1.060	1.035
Final *R* indices [$I > 2\sigma(I)$]	$R_1 = 0.0195$, $wR_2 = 0.0475$	$R_1 = 0.0335$, $wR_2 = 0.0636$	$R_1 = 0.0488$, $wR_2 = 0.1022$
R indices (all data)	$R_1 = 0.0213$, $wR_2 = 0.0482$	$R_1 = 0.0397$, $wR_2 = 0.0662$	$R_1 = 0.0875$, $wR_2 = 0.1170$
Largest diff. peak and hole/e. Å^{-3}	0.919 and -0.415	1.568 and -1.329	0.515 and -0.415

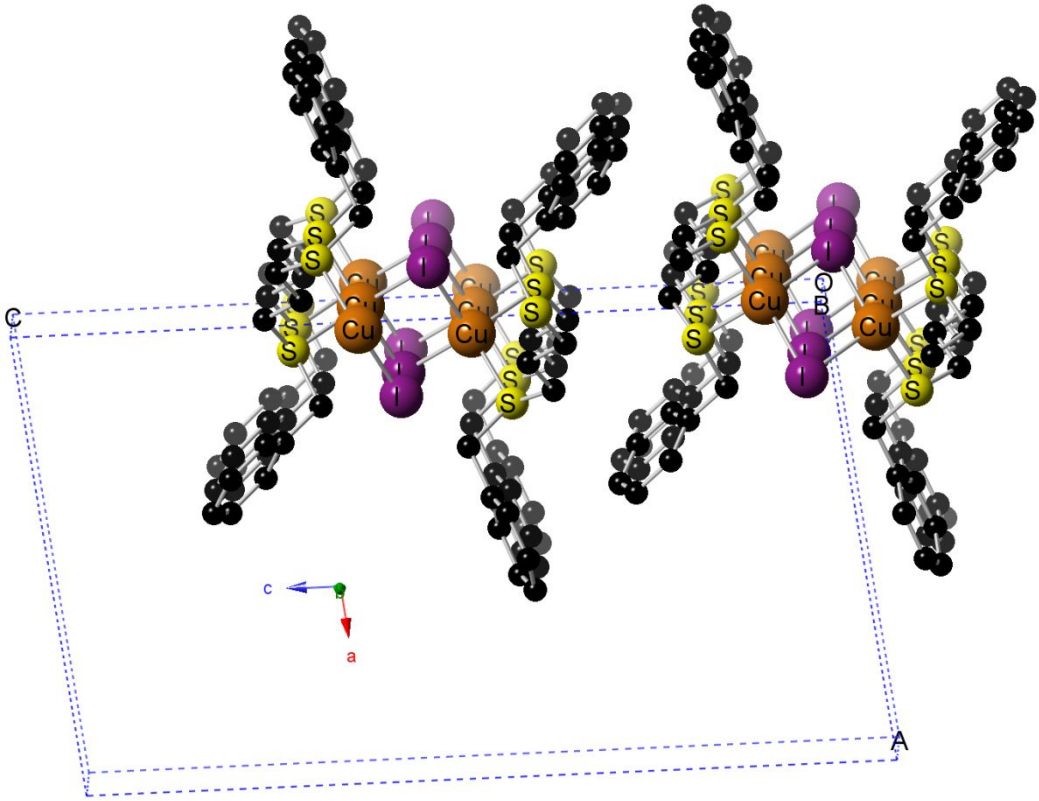

Figure S1. Relative orientation of the ribbons in the packing of **CP4** running along the *c* axis.

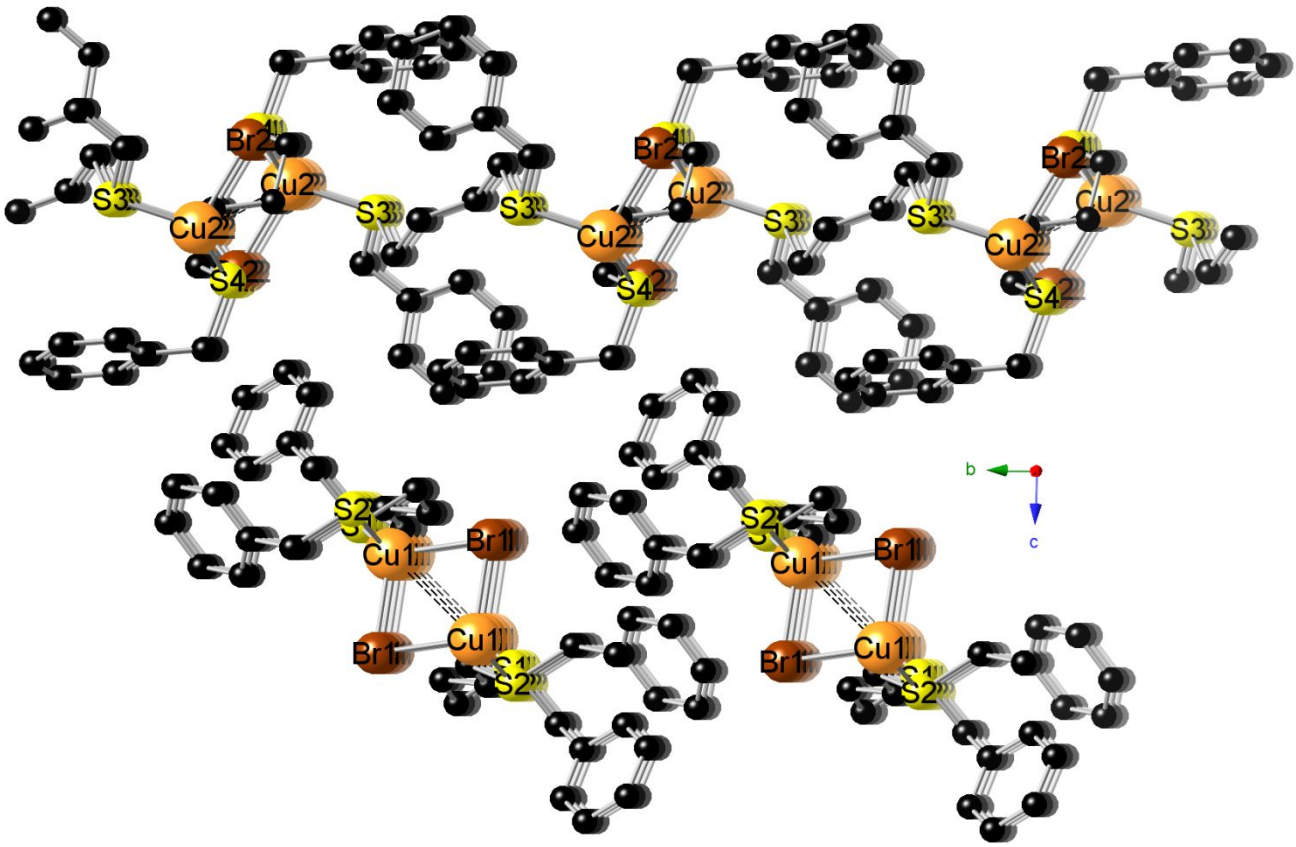

Figure S2. View of **CP9-1D** (bottom) and **CP9-2D** (top) within the same unit cell along the *b* axis.

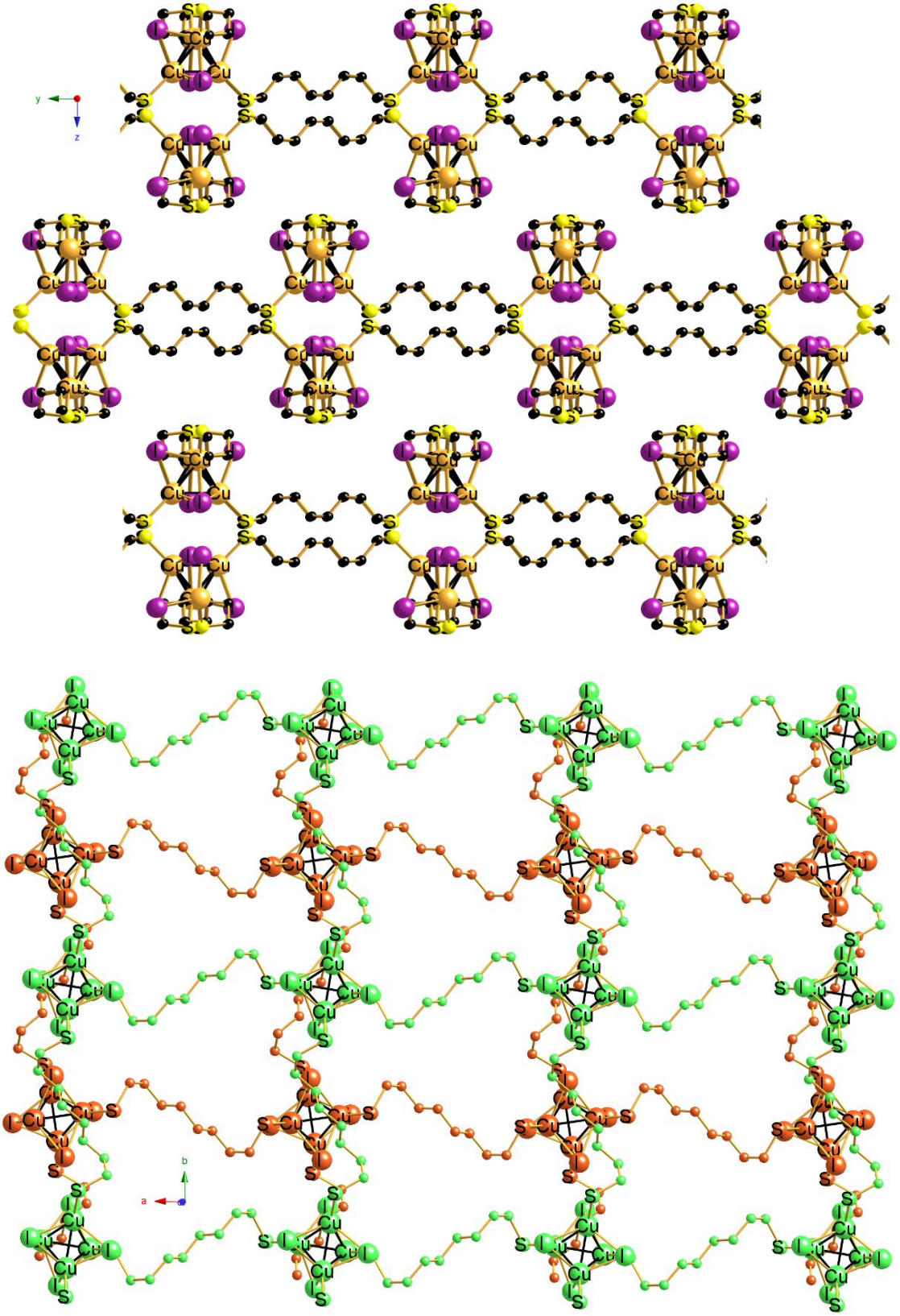

Figure S3. (Top) View down the *c* axis showing the superposition of two *ab* layers of **CP18**. (Bottom) View down the *a* axis showing the arrangement of the layers **CP18** on the *bc* plane. tetragonal space group I-4 2 d

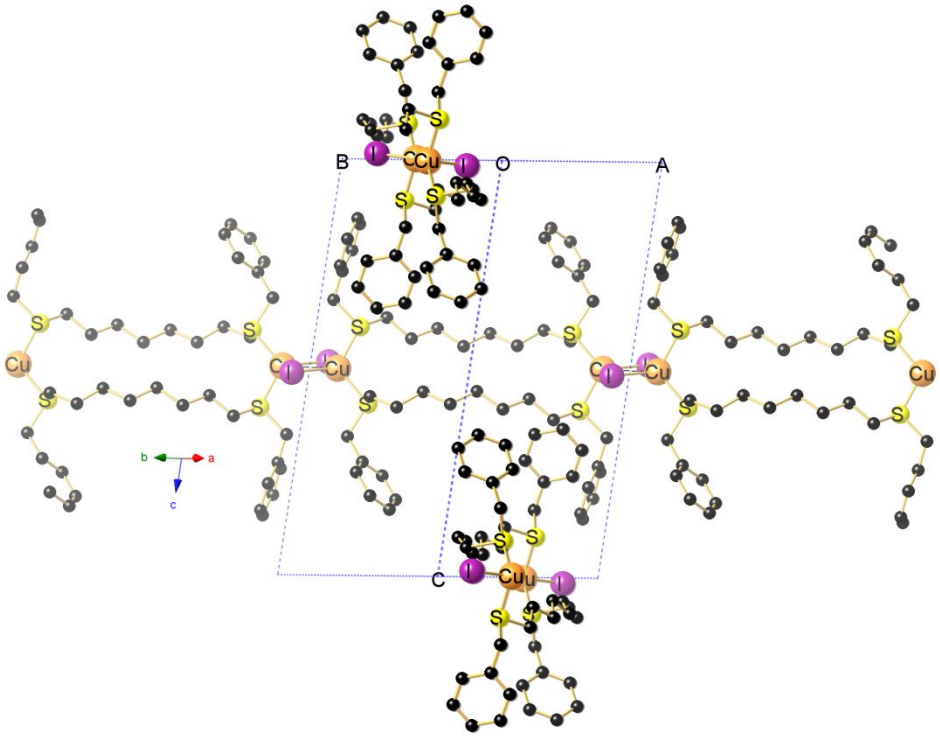

Figure S4. View of the ribbons of **CP19** arranged in an orthogonal manner in an *ABAB* sequence.

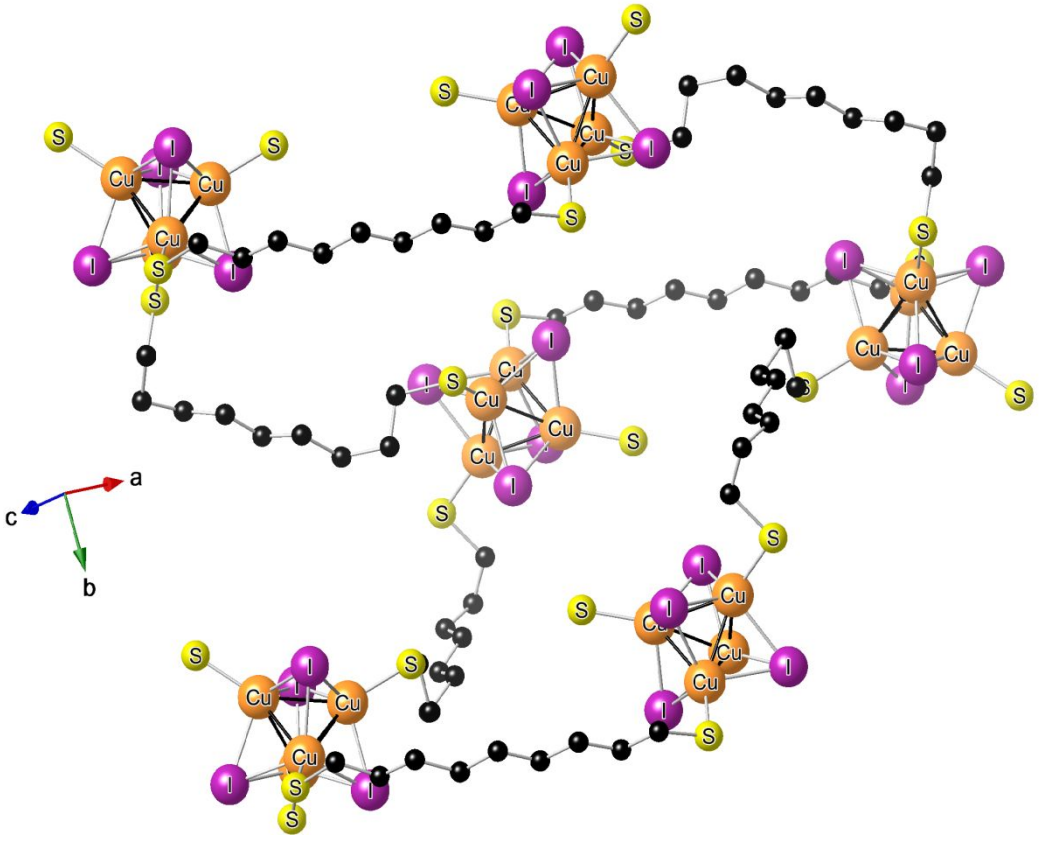

Figure S5. View of two distorted square rings almost perpendicularly orientated with respect to other one making part of the 2D network of **CP22**.

Powder X-Ray diffractions

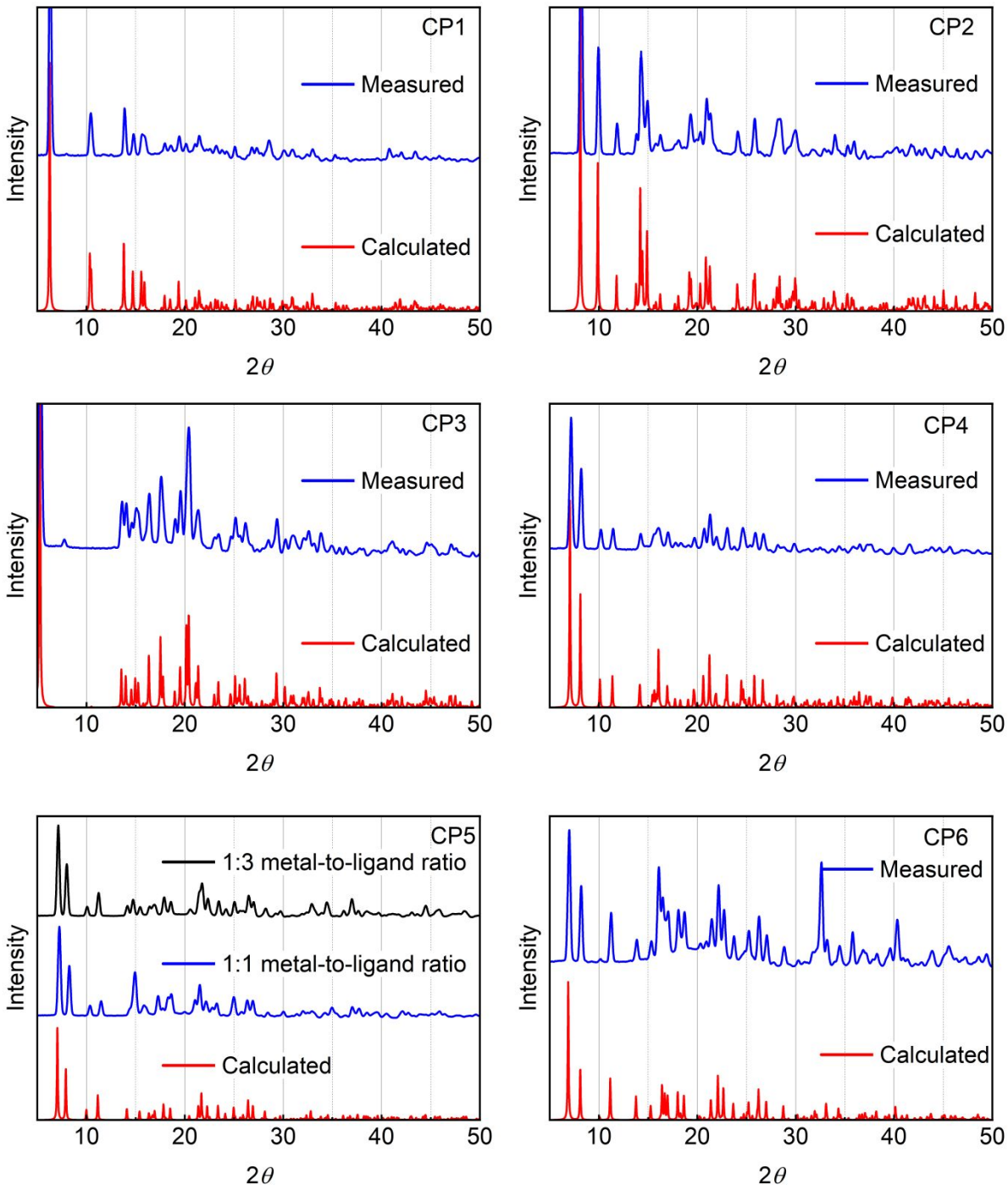

Figure S6. Powder X-ray diffraction patterns calculated (red) and experimental (blue) for **CP1-6** at 173 K. The calculated and measured diffraction patterns match well with each other, confirming the homogeneity of the crystalline phases.

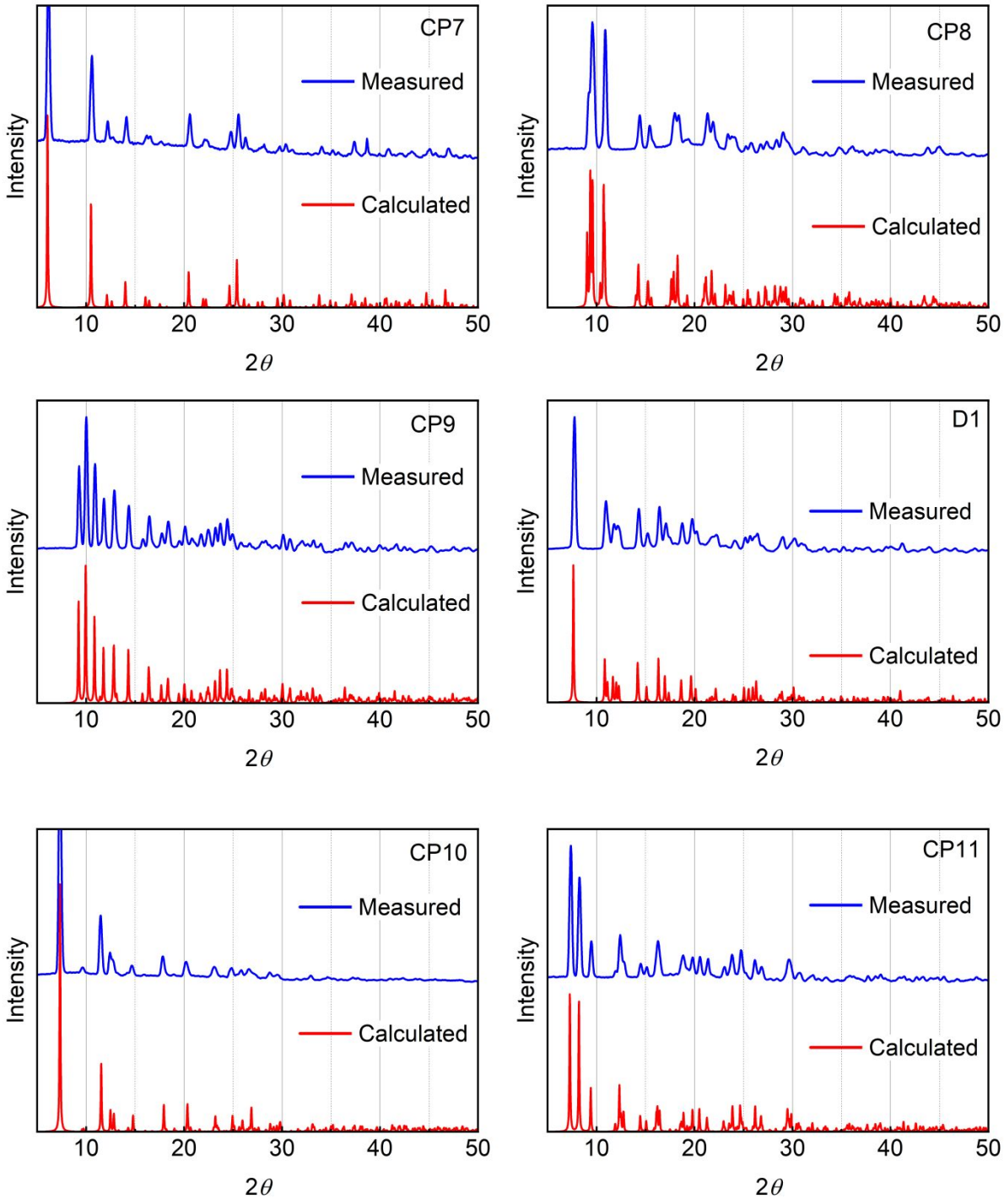

Figure S7. Powder X-ray diffraction patterns calculated (red) and experimental (blue) for **D1** and **CP7-11** at 173 K. The calculated and measured diffraction patterns match well with each other, confirming the homogeneity of the crystalline phases.

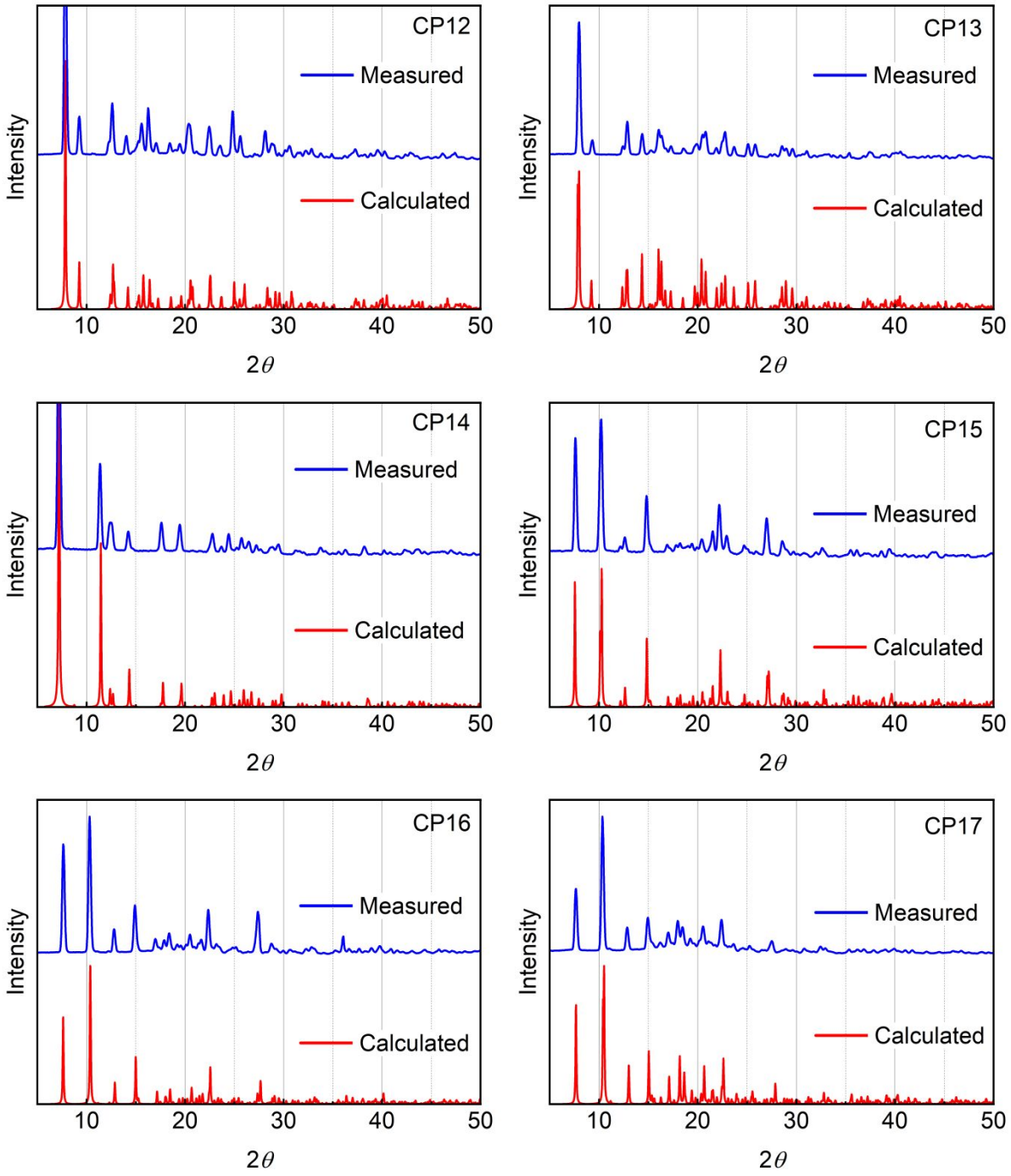

Figure S8. Powder X-ray diffraction patterns calculated (red) and experimental (blue) for **CP12-17** at 173 K. The calculated and measured diffraction patterns match well with each other, confirming the homogeneity of the crystalline phases.

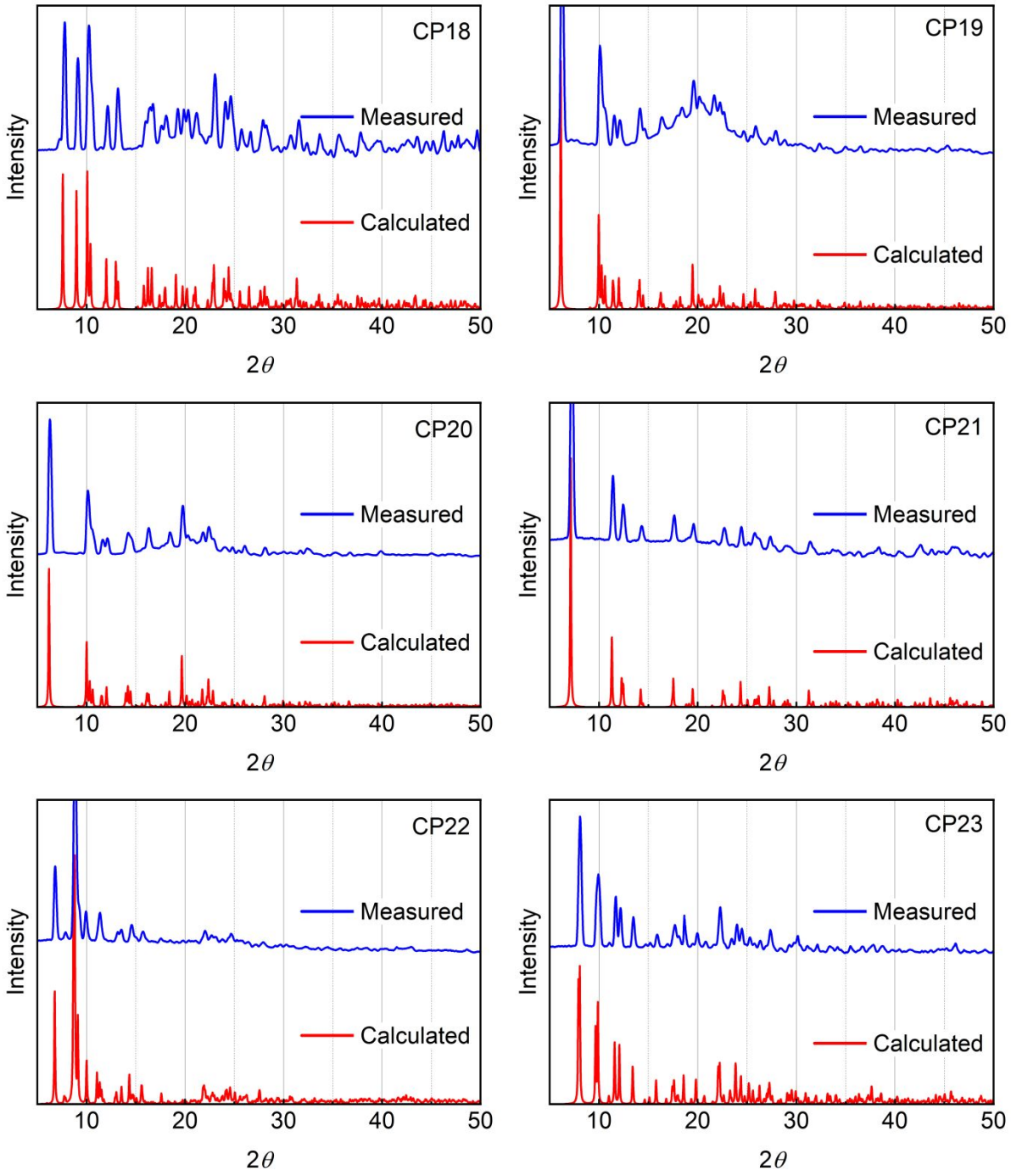

Figure S9. Powder X-ray diffraction patterns calculated (red) and experimental (blue) for **CP18-23** at 173 K. The calculated and measured diffraction patterns match well with each other, confirming the homogeneity of the crystalline phases except for **CP19** which might be cause by solvent molecule or amorphous phase in the oil matrix used.

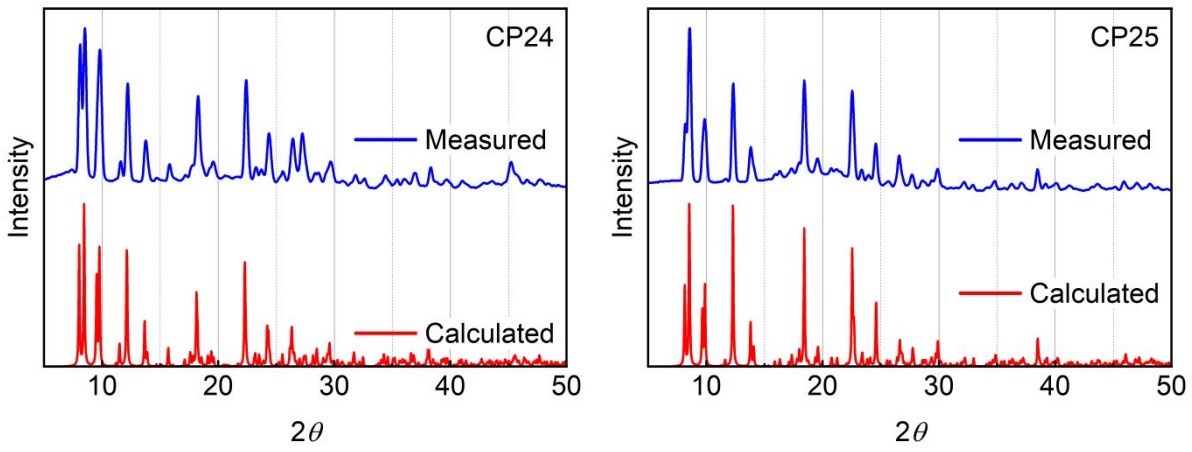

Figure S10. Powder X-ray diffraction patterns calculated (red) and experimental (blue) for **CP24-25** at 173 K. The calculated and measured diffraction patterns match well with each other, confirming the homogeneity of the crystalline phases.

Thermogravimetric analysis

Table S6. TGA data.

	Formula [*M* (g.mol^{-1})]	***T* at dTG_{max} (°C)**	**$^{Exp}\Delta m$ (%)**	**$^{Calc}\Delta m$ (%)**	**Attribution**
CP1	$C_{15}H_{16}CuIS_2$ [450.84]	268 835	-55.95 -36.89	-57.76 -35.20	**L1** I + 0.5 Cu
CP2	$C_{15}H_{16}BrCuS_2$ [403.85]	277 860	-61.33 -17.30	-64.48 -17.76	**L1** 0.75 Br + 0.25 Cu
CP3	$C_{15}H_{16}ClCuS_2$ [359.42]	270 887	-53.70 -33.04	-54.34	0.75 **L1** 0.25 **L1** + Cl + 0.25 Cu
CP4	$C_{17}H_{20}CuIS_2$ [478.89]	294 868	-53.07 -32.72	-54.21 -32.52	0.9 **L2** 0.1 **L2** + I
CP5	$C_{17}H_{20}BrCuS_2$ [431.90]	283 449	-61.21 -13.81	-60.12 -15.93	0.9 **L2** 0.1 **L2** + 0.5 Br
CP6	$C_{17}H_{20}S_2ClCu$ [387.44]	279	-65.38	-67.21	**L2**
CP7	$C_{27}H_{33}Cu_4I_4S_3$ [1215.47]	266 870	-37.69 -50.09	-37.33 -52.22	1.5 **L3** 4 I + 2 Cu
CP8	$C_{36}H_{44}Cu_2I_2S_4$ [985.83]	262 770	-65.16 -29.09	-67.80 -28.98	**L3** + 0.5 I 1.5 Cu + 1.5 I
CP9	$C_{18}H_{22}BrCuS_2$ [445.92]	244	-80.31	-82.09	**L3** + Cu
D1	$C_{36}H_{44}Cl_2Cu_2S_4$ [802.93]	246	-76.01	-75.35	2 **L3**
CP10	$C_{40}H_{52}Cu_4I_4S_4$ [1422.81]	280 375 874	-41.42 -4.34 -41.67	-46.46 -4.46 -40.14	2 **L4** 0.5 I 3.5 I + 2 Cu
CP11	$C_{20}H_{26}CuIS_2$ [520.97]	272 819	-63.73 -20.09	63.45 -24.36	**L4** I
CP12	$C_{20}H_{26}BrCuS_2$ [473.98]	272 430 453	-60.08 -14.20 -7.03	-69.74 -13.41 -8.4	**L4** Cu Br
CP13	$C_{20}H_{26}ClCuS_2$ [429.52]	277	-77.10	-76.96	**L4**
CP14	$C_{42}H_{56}Cu_4I_4S_4$ [1450.86]	282 820	-47.73 -38.00	-47.50 -39.37	2 **L5** 4 I + Cu
CP15	$C_{21}H_{28}CuIS_2$ [534.99]	312 686	-64.95 -30.70	-64.41 -29.66	**L5** I + 0.5 Cu
CP16	$C_{21}H_{28}BrCuS_2$ [488.00]	308 433	-64.70 -16.41	-70.61 -16.37	**L5** Br
CP17	$C_{21}H_{28}ClCuS_2$ [443.54]	296	-78.67	-77.69	**L5**
CP18	$C_{44}H_{60}Cu_4I_4S_4$ [1478.92]	301 784	-49.25 -34.77	-48.49 -34.33	2 **L6** 3.5 I + Cu
CP19	$C_{22}H_{30}CuIS_2$ [549.02]	276	-87.23	-88.43	**L5** + I
CP20	$C_{44}H_{60}Br_2Cu_2S_4$ [1004.06]	288 397	-65.51 -16.49	-71.43 -15.92	**L6** 2 Br
CP21	$C_{44}H_{60}Cl_2Cu_2S_4$ [915.14]	298	-78.78	-78.37	2 **L6**
CP22	$C_{92}H_{128}Cu_8I_8S_8$ [3013.94]	281 850	-53.25 -35.84	-49.45 -35.80	4 **L7** 7 I + 3 Cu
CP23	$C_{23}H_{32}Cu_2I_2S$ [753.53]	280 836	-44.09 -39.96	-49.45 -33.68	**L7** 2 I
CP24	$C_{23}H_{32}BrCuS_2$ [516.05]	279	-76.5	-72.21	**L7**
CP25	$C_{23}H_{32}ClCuS_2$ [471.59]	288	-80.94	-79.02	**L7**

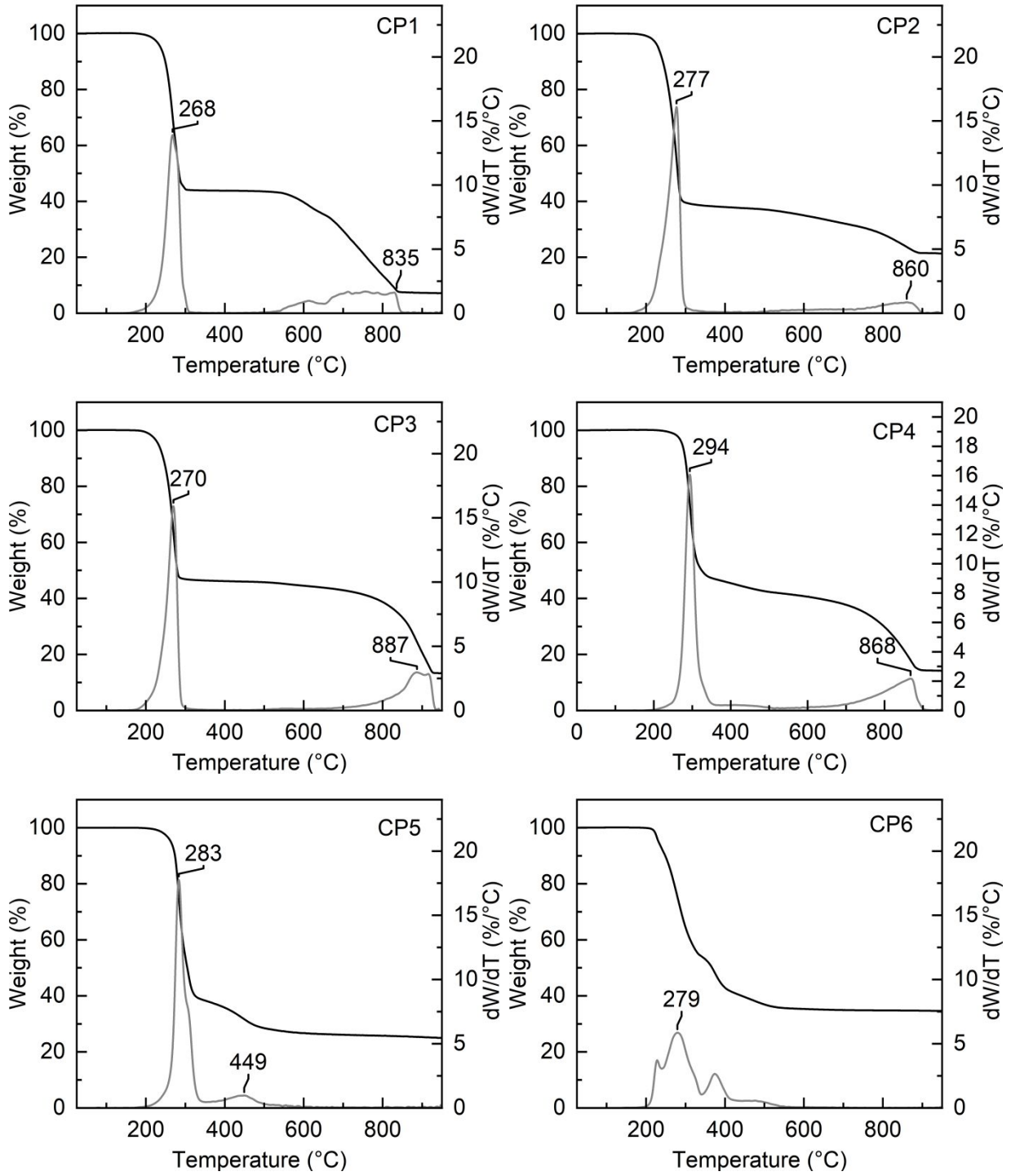

Figure S11. TGA (black) and first derivative (grey) of **CP1-6** recorded under argon atmosphere T = [25°C – 950°C].

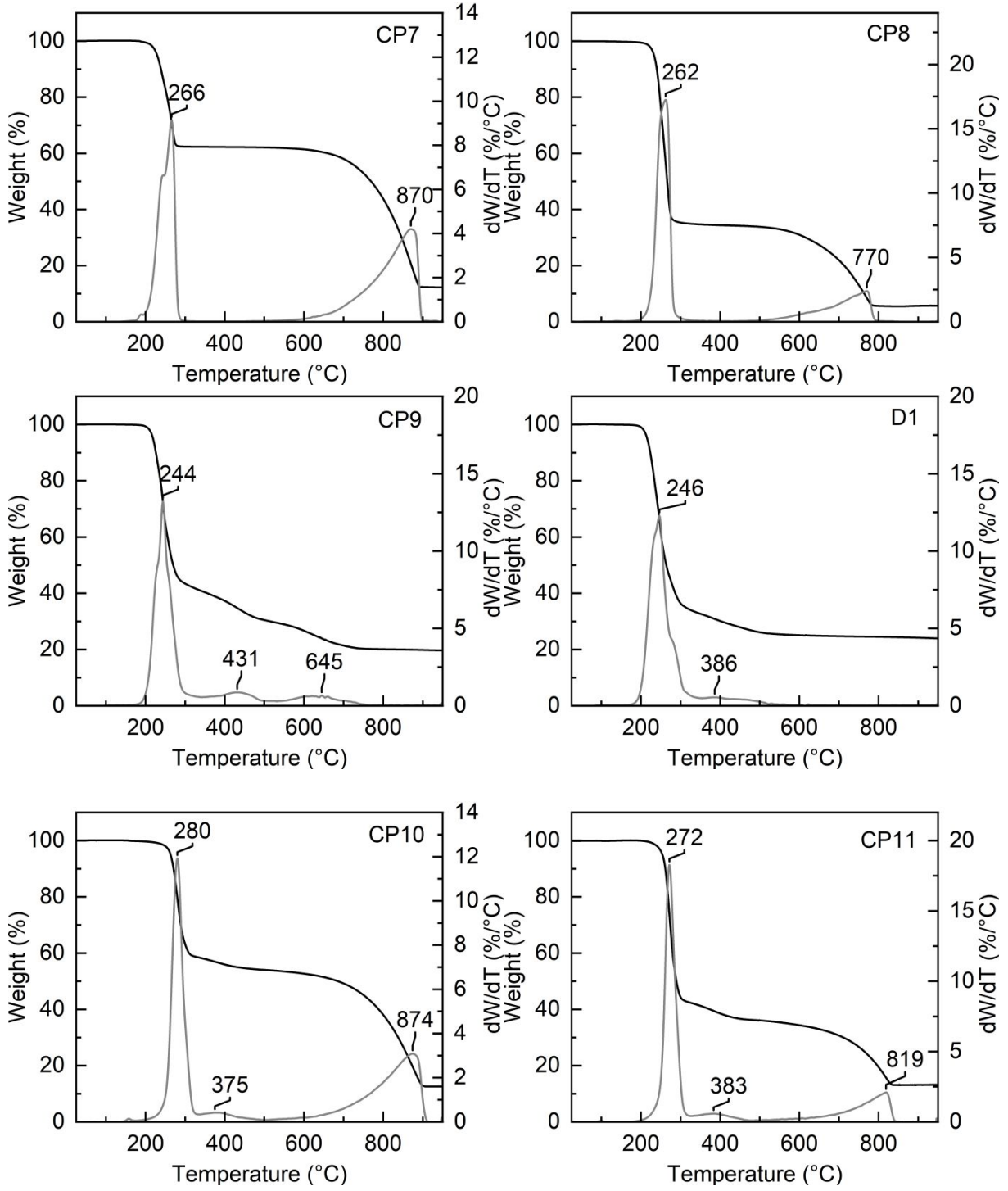

Figure S12. TGA (black) and first derivative (grey) of **D1** and **CP7-11** recorded under argon atmosphere T = [25°C – 950°C].

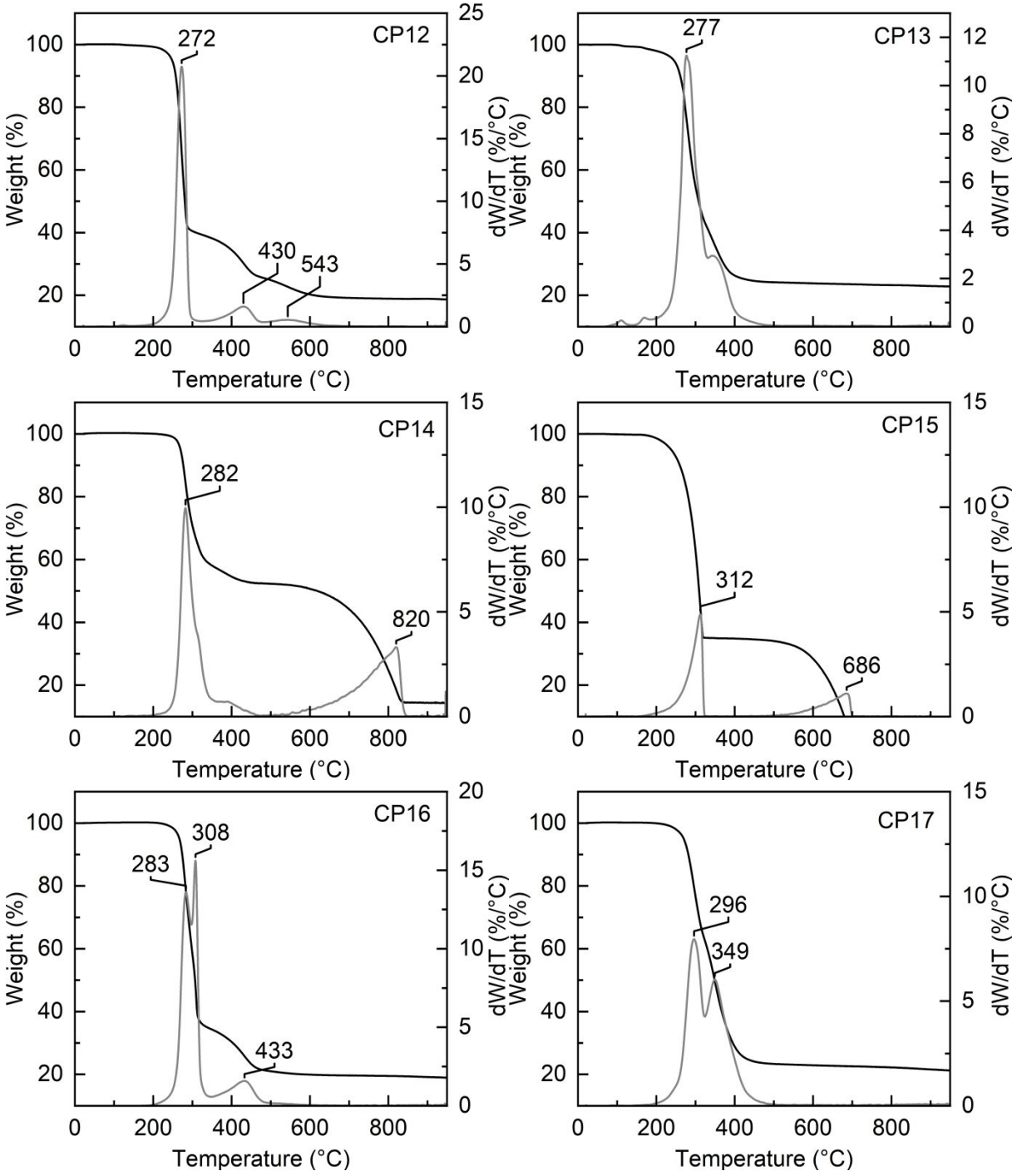

Figure S13. TGA (black) and first derivative (grey) of **CP12-17** recorded under argon atmosphere T = [25°C – 950°C].

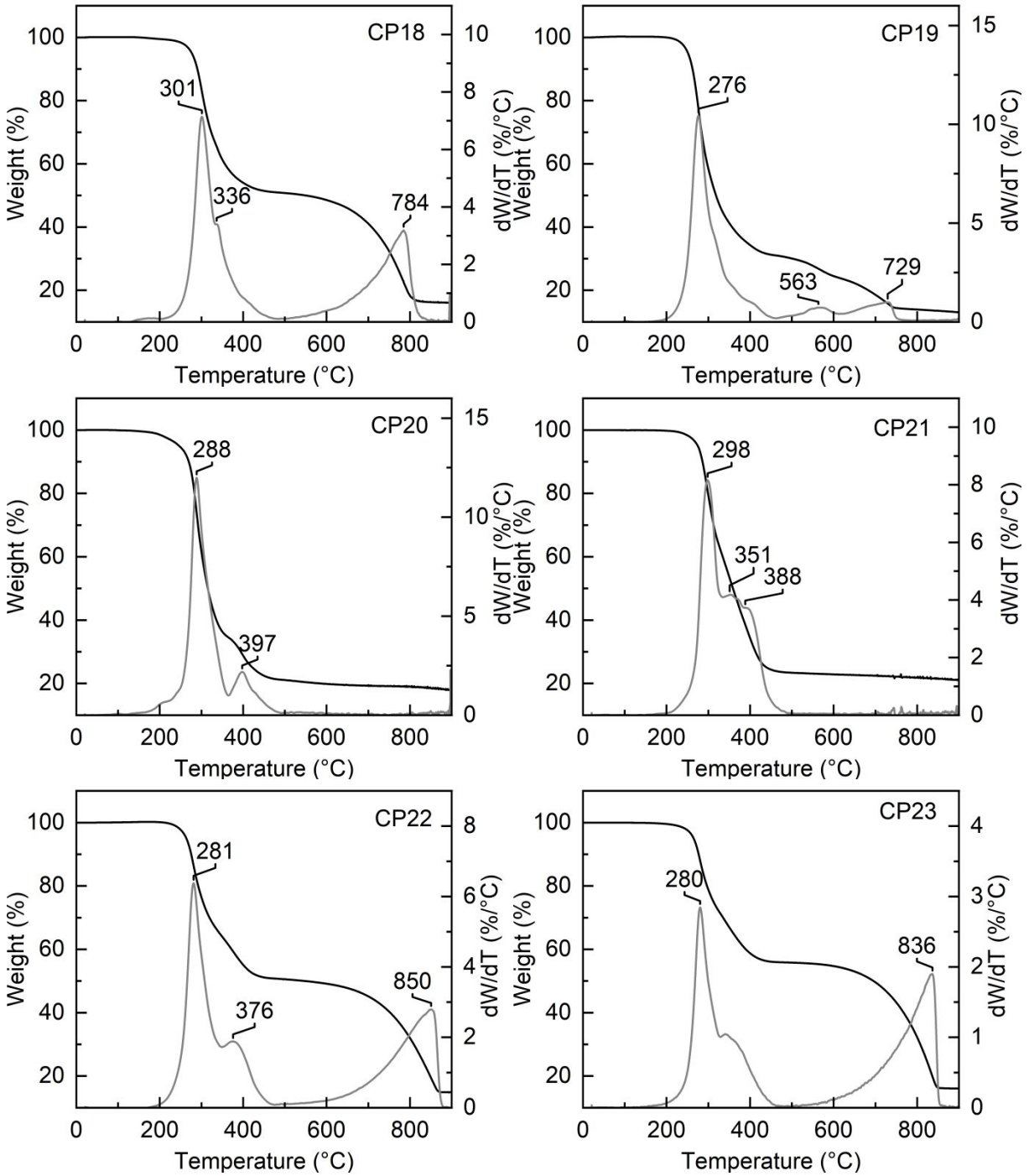

Figure S14. TGA (black) and first derivative (grey) of **CP18-23** recorded under argon atmosphere T = [25°C – 950°C].

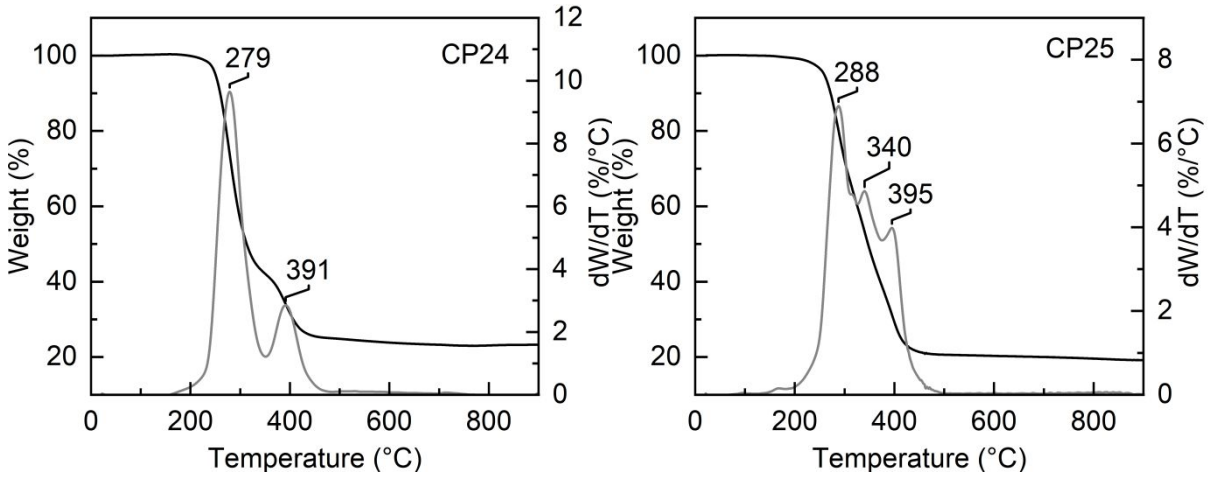

Figure S15. TGA (black) and first derivative (grey) of **CP24-25** recorded under argon atmosphere T = [25°C – 950°C].

Infrared and Raman

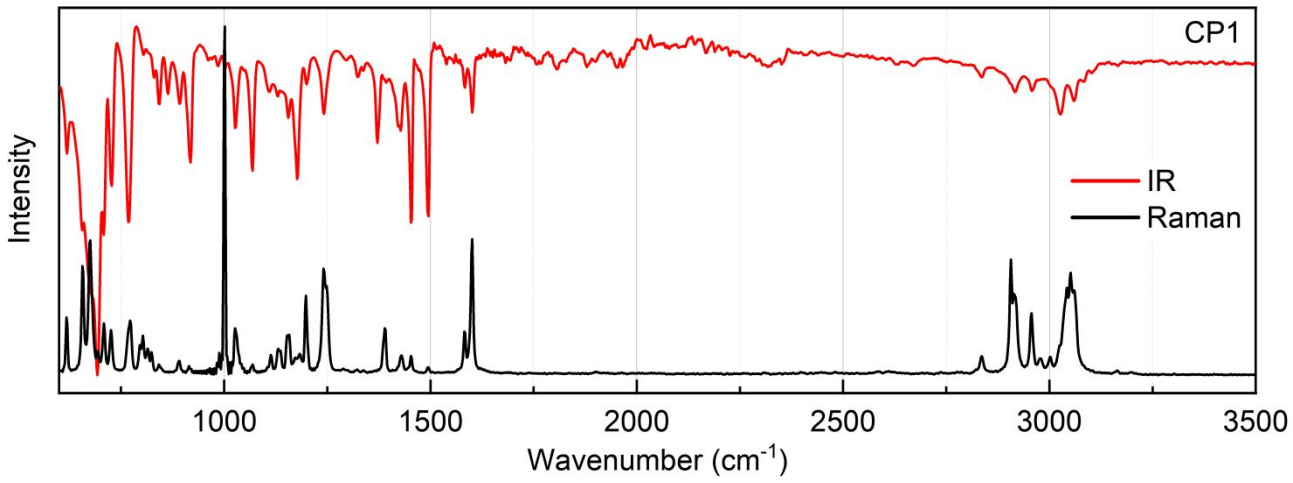

Figure S16. Solid state Raman and IR spectrum of **CP1**.

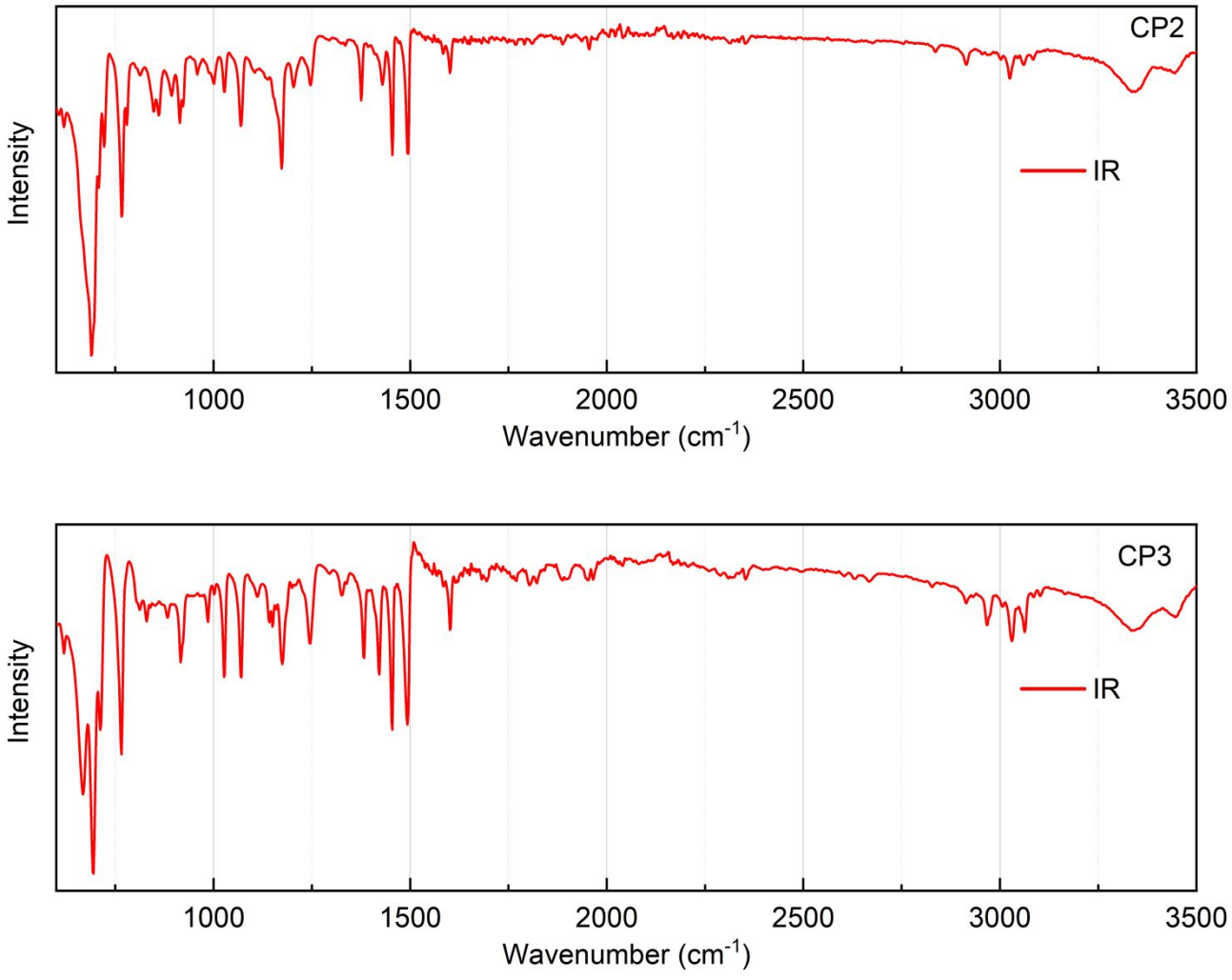

Figure S17. Solid state IR spectrum of **CP2** and **CP3**.

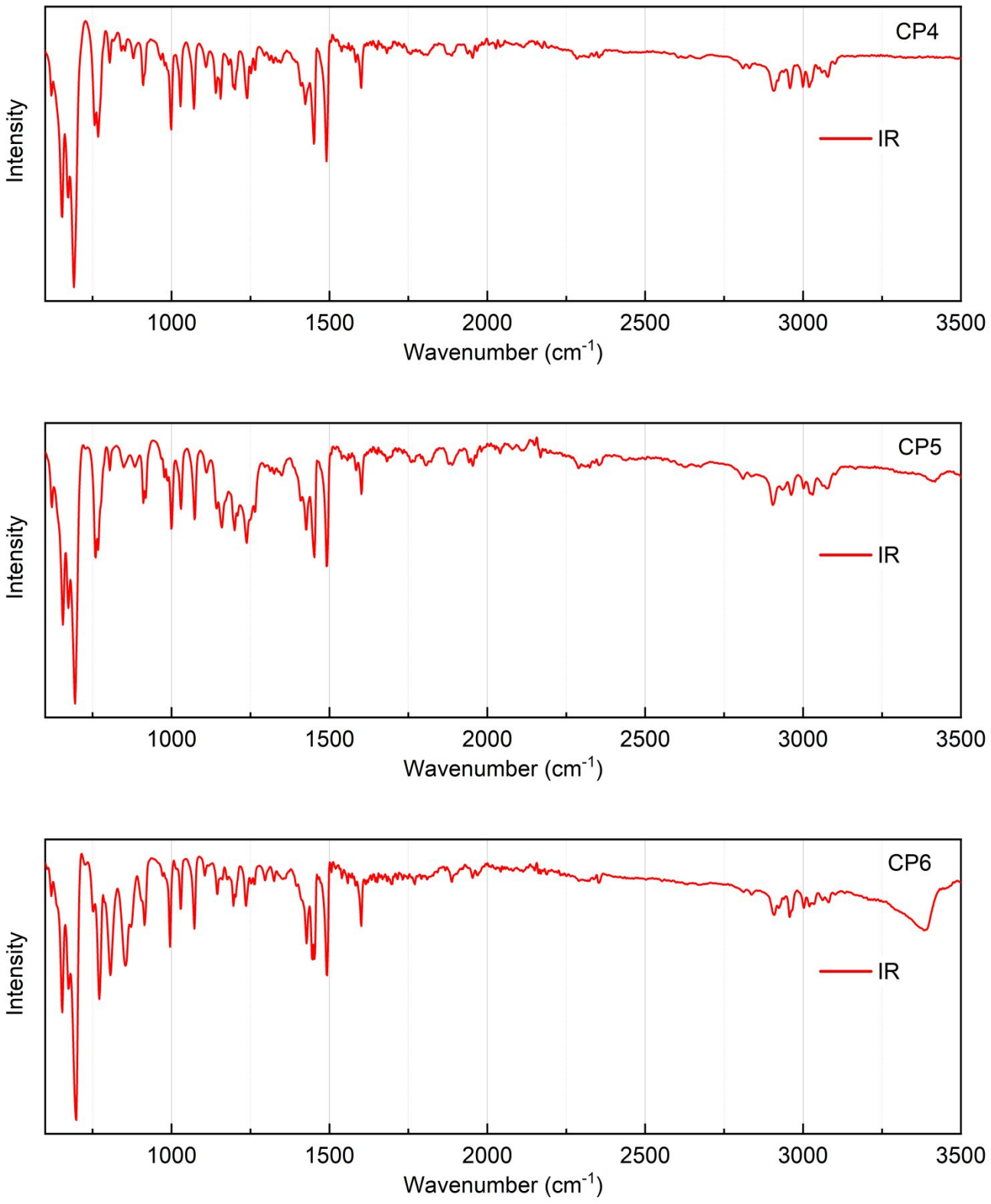

Figure S18. Solid state IR spectrum of **CP4-6**.

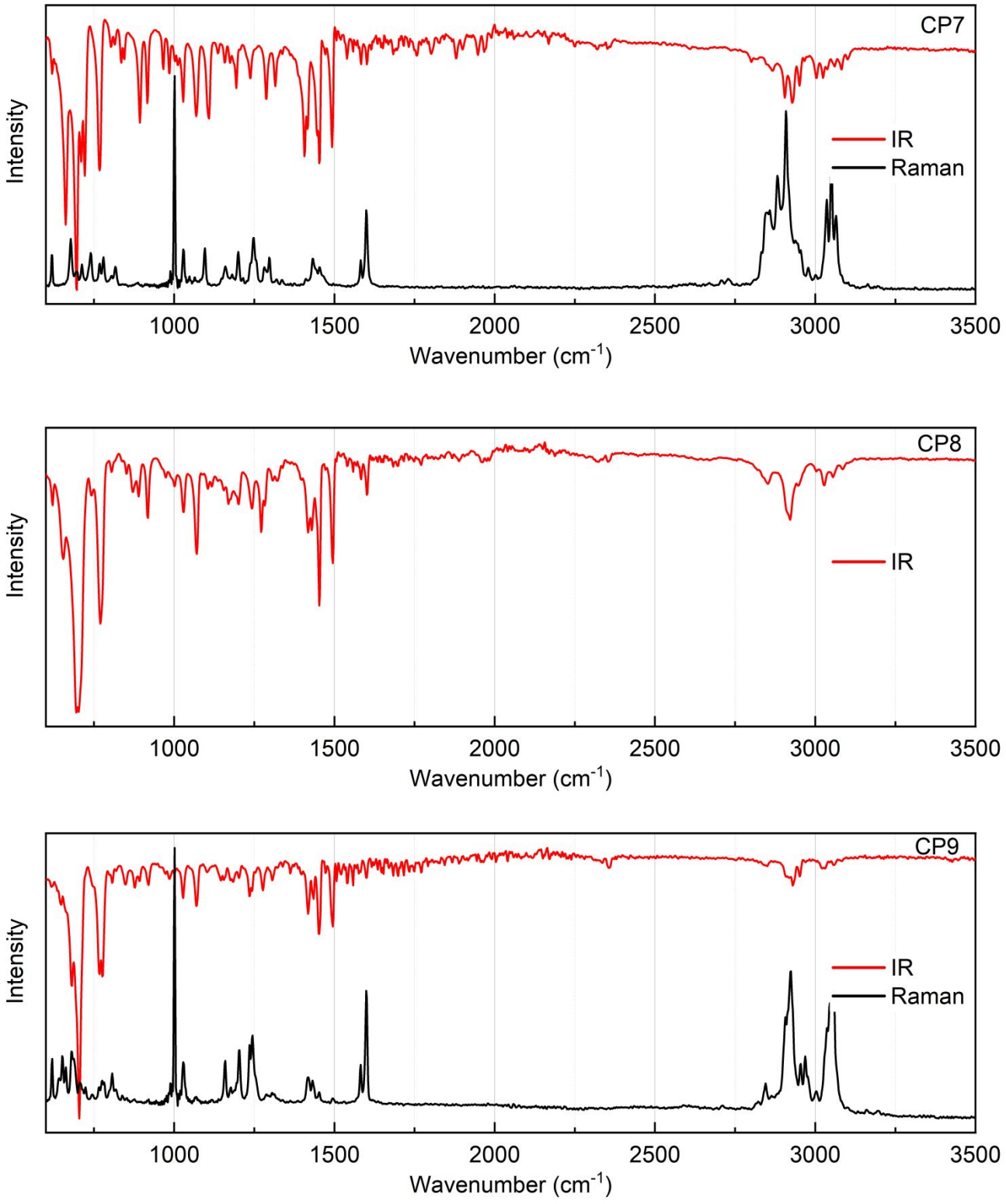

Figure S19. Solid state IR spectrum of **CP7-9** and Raman of **CP8**.

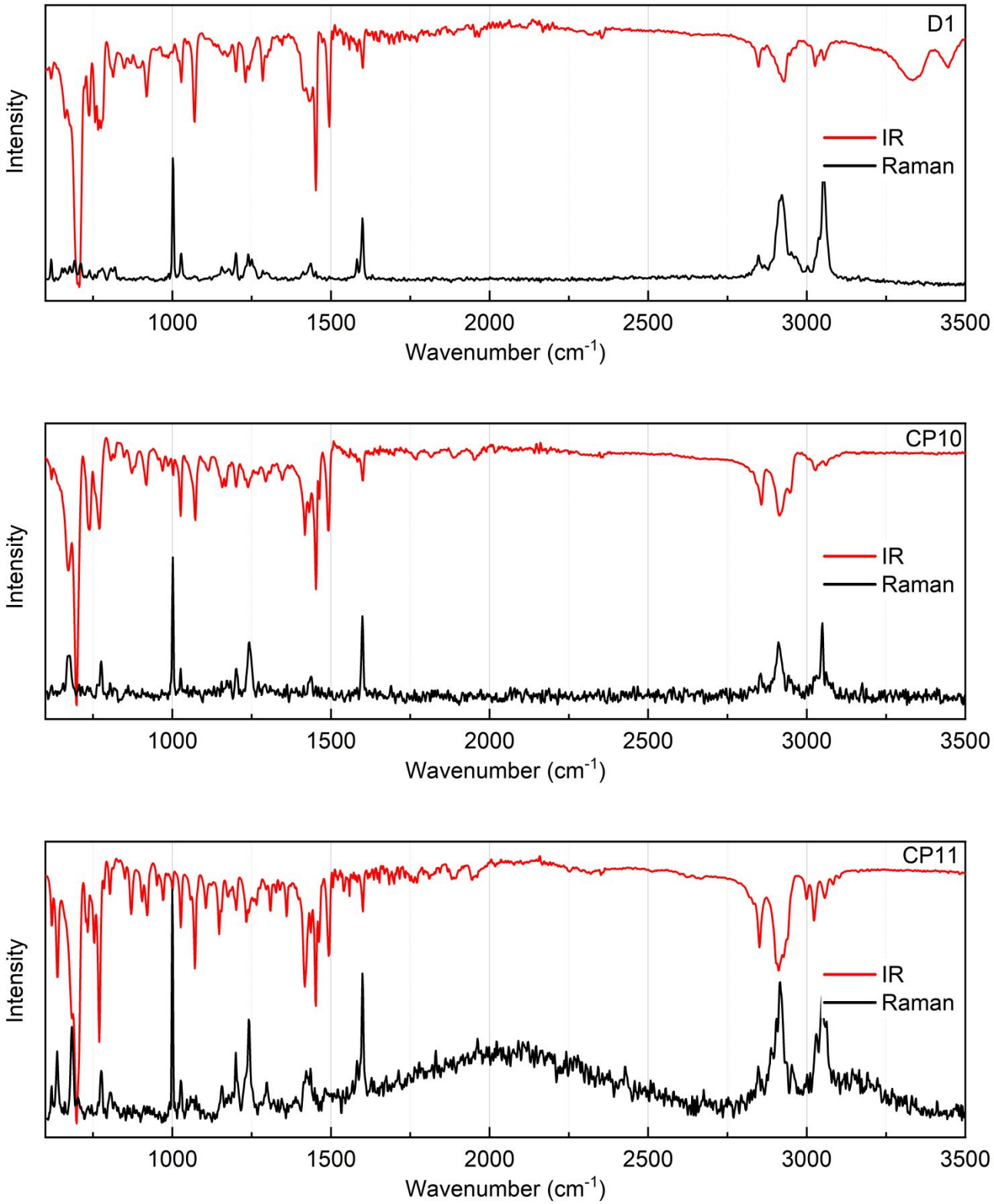

Figure S20. Solid state IR and Raman spectrum of **CP10-11 and D1**.

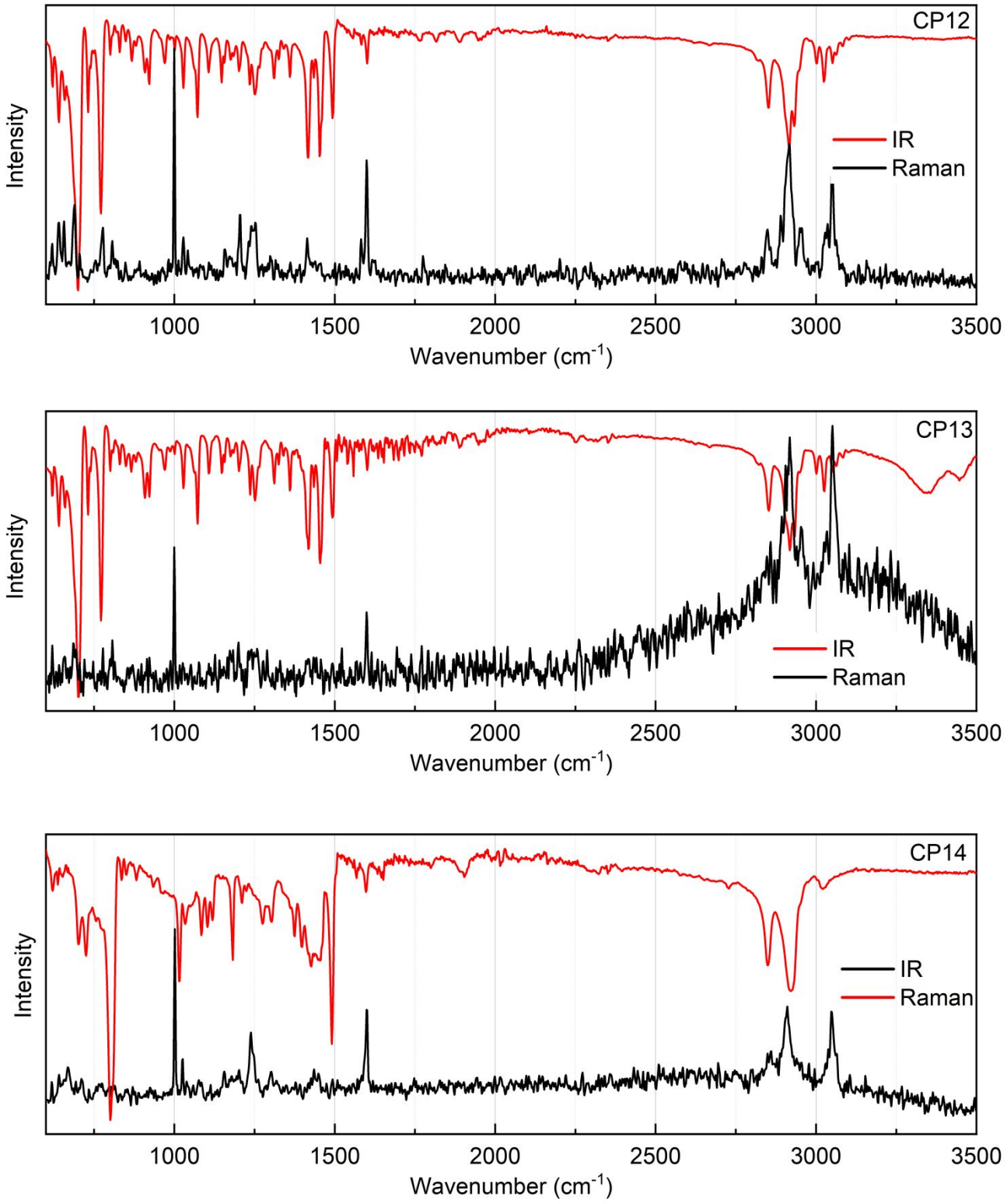

Figure S21. Solid state IR and Raman spectrum of **CP12-14**.

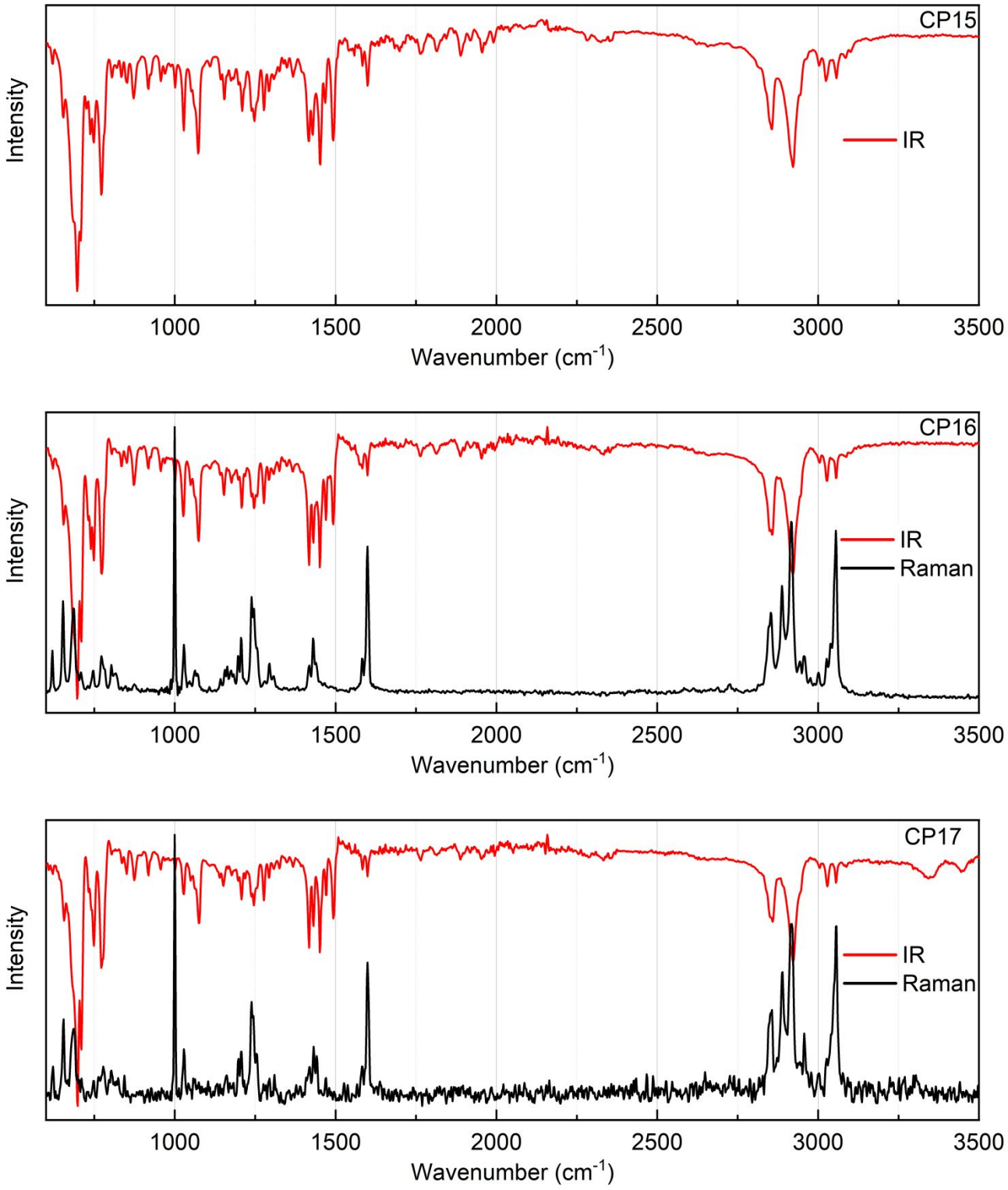

Figure S22. Solid state IR spectrum of **CP15-17** and Raman of **CP15** and **17**.

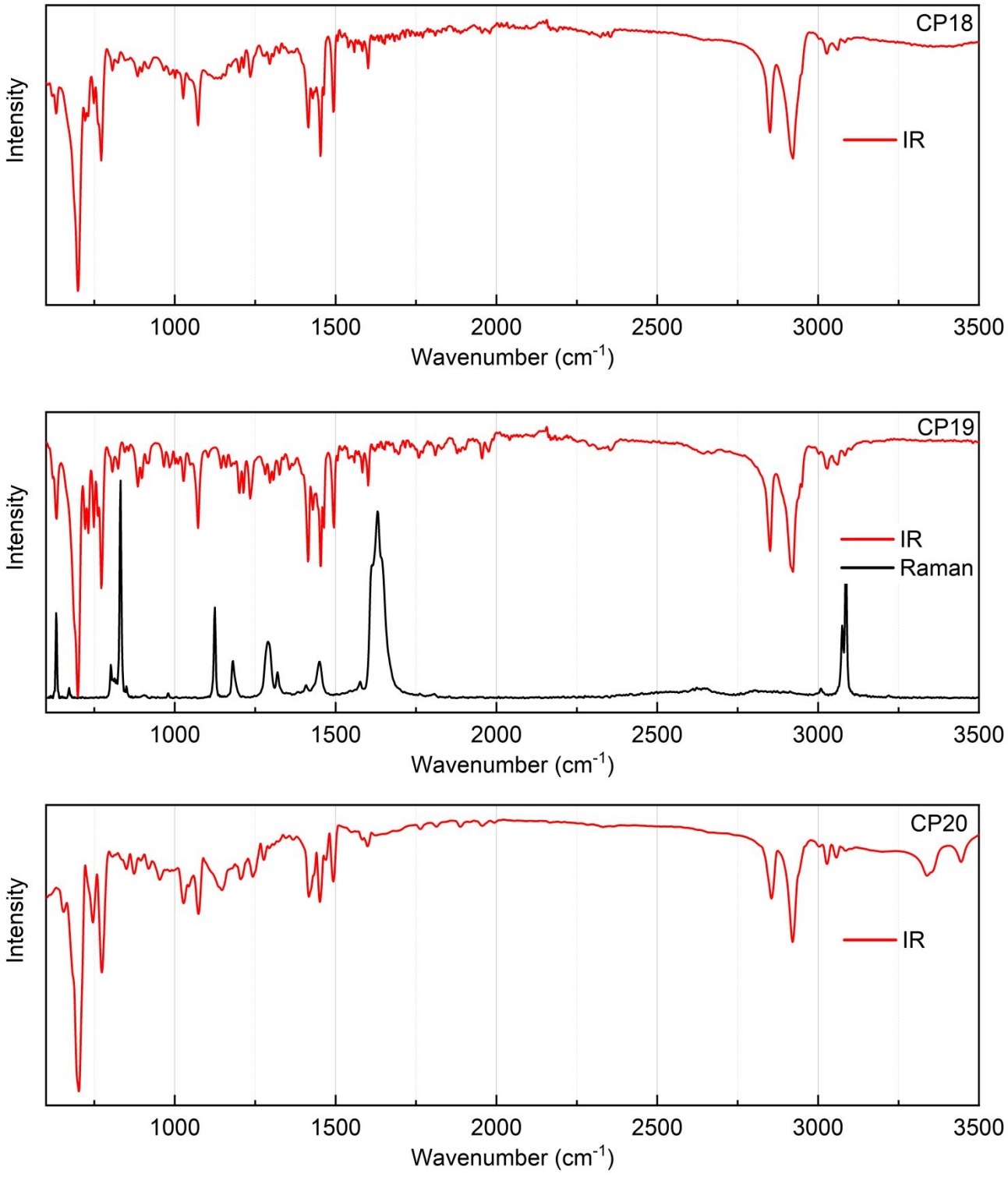

Figure S23. Solid state IR spectrum of **CP18-20** and Raman of **CP19**.

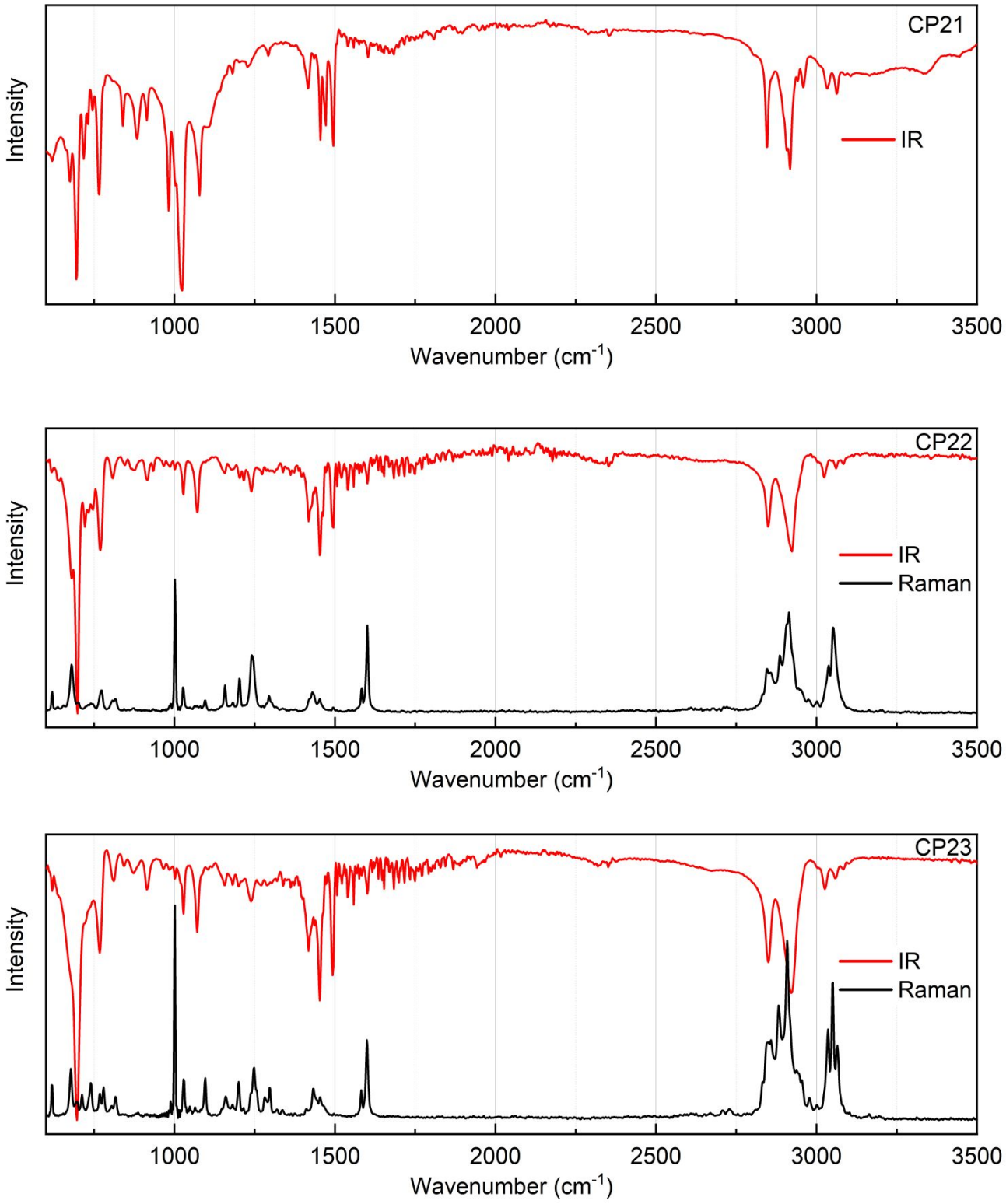

Figure S24. Solid state IR spectrum of **CP21-23** and Raman of **CP22,23**.

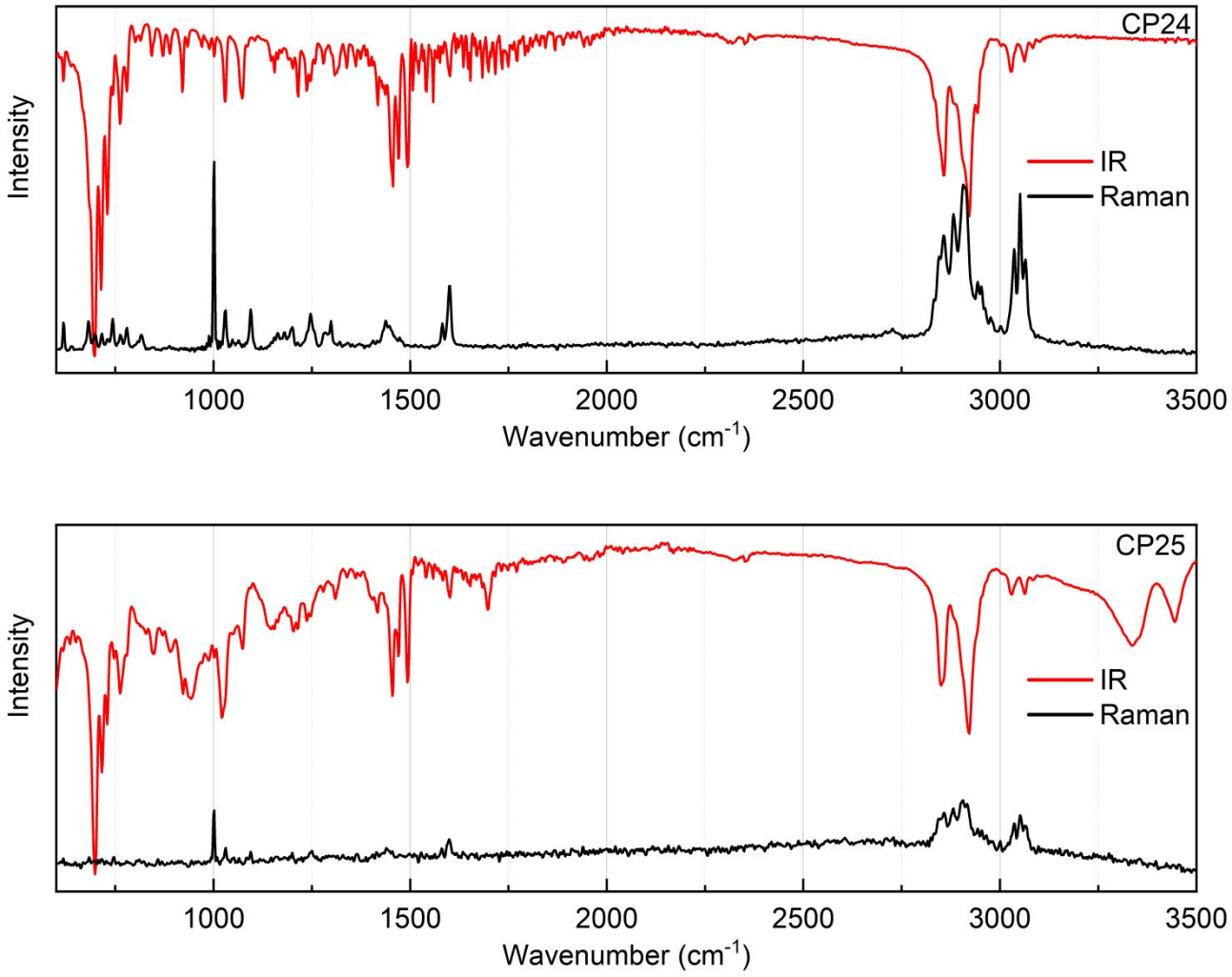

Figure S25. Solid state IR and Raman spectrum of **CP24** and **CP25**.

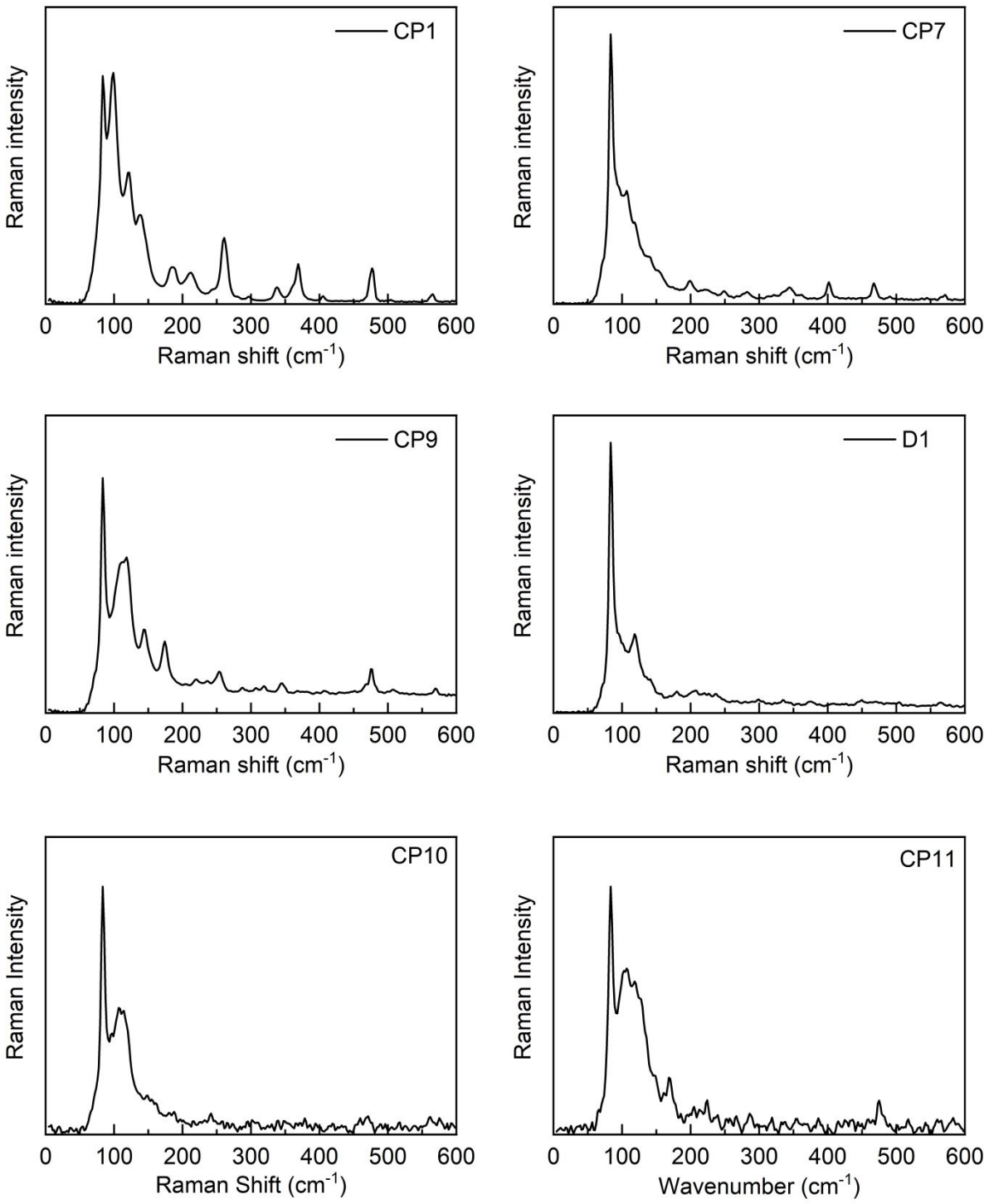

Figure S26. Expansion of solid-state Raman spectrum in the region characteristic of the cluster skeleton modes of **CP1, 7, 9-11** and **D1**.

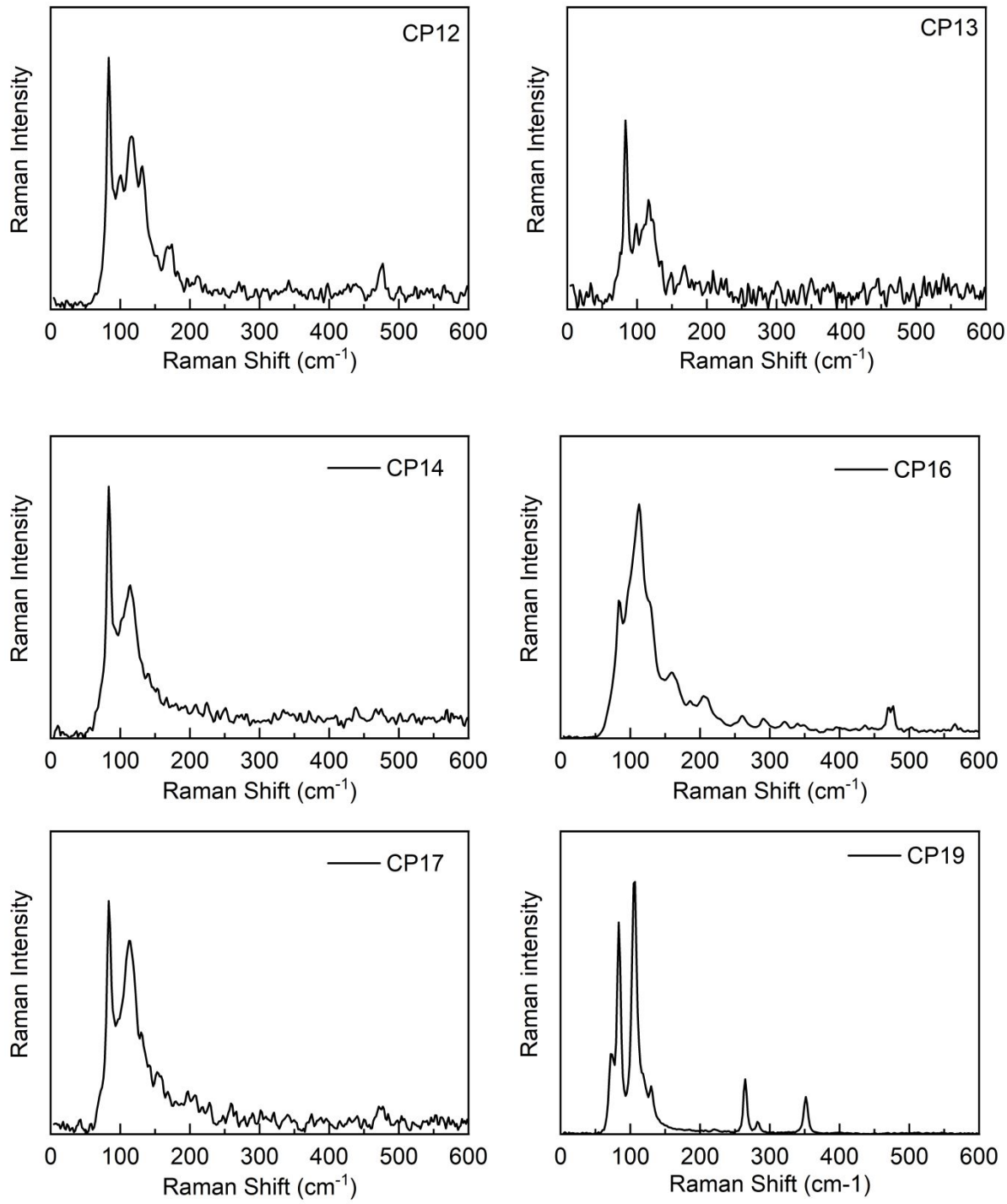

Figure S27. Expansion of solid state Raman spectrum in the region characteristic of the cluster skeleton modes of **CP12-14, 16-17** and **19**.

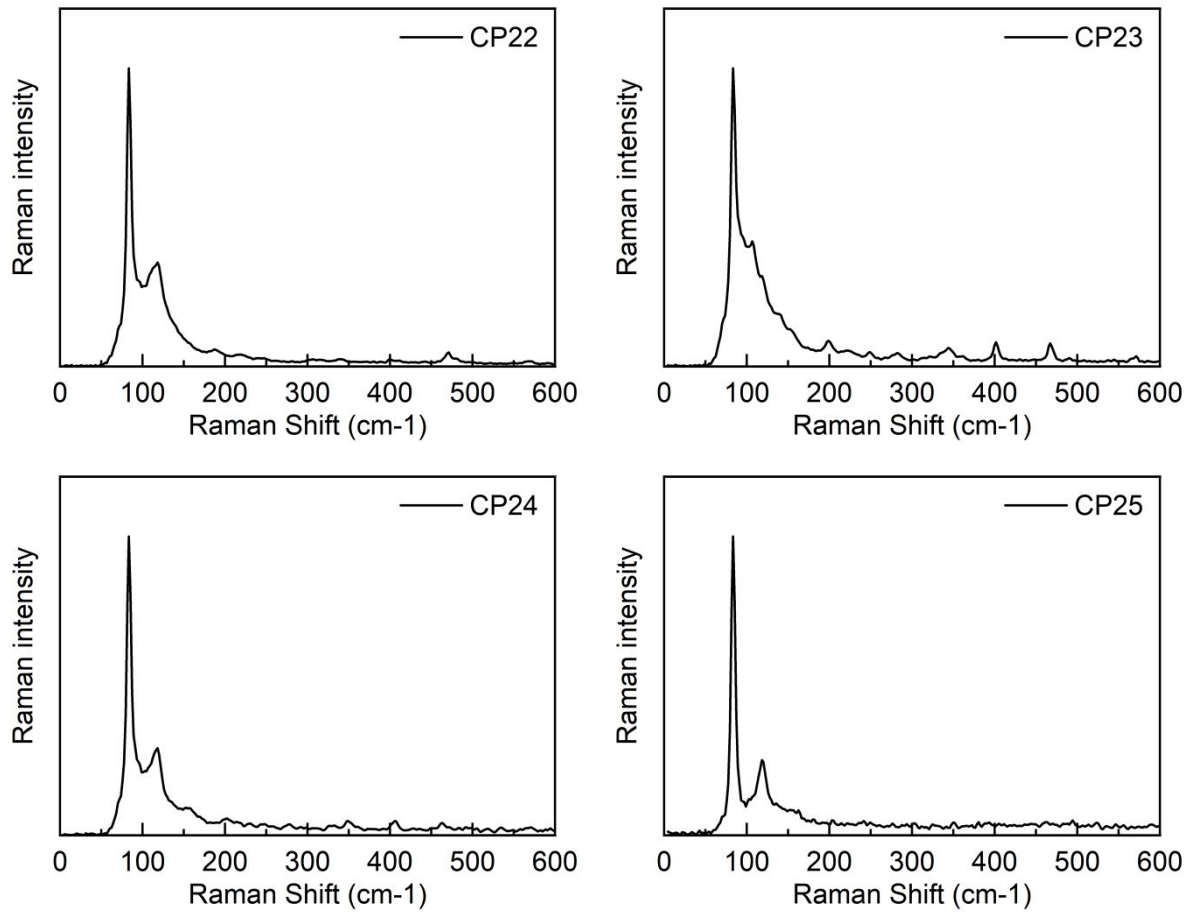

Figure S28. Expansion of solid-state Raman spectrum in the region characteristic of the cluster skeleton modes of **CP22-25**.

Absorption, Excitation and Emission

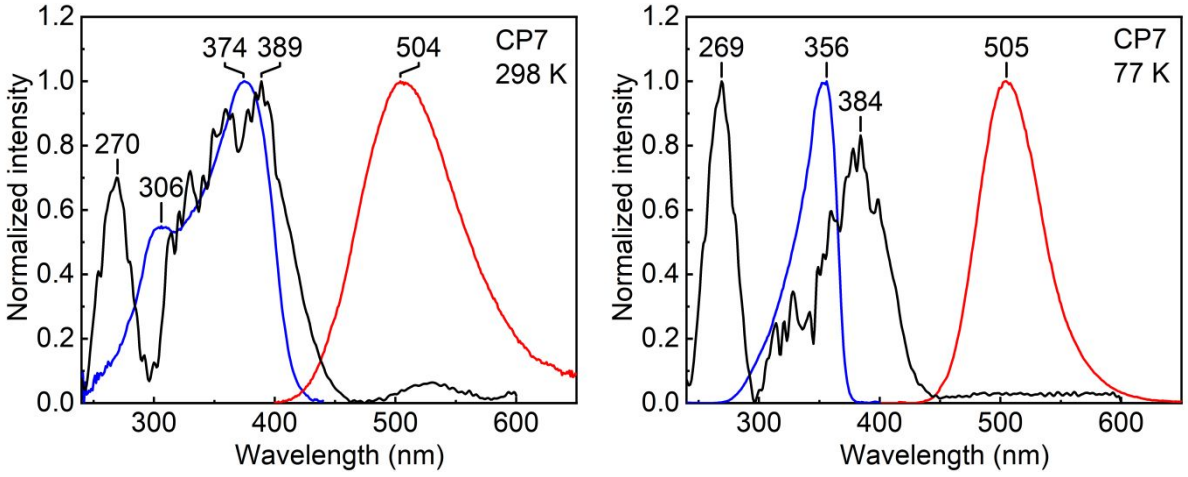

Figure S29. Solid-state absorption (black), emission (red) and excitation (blue) spectra for **CP7** at 298 K (left, λ_{ex} = 370 nm, λ_{em} = 500 nm) and 77 K (right, λ_{ex} =350 nm, λ_{em} = 500 nm).

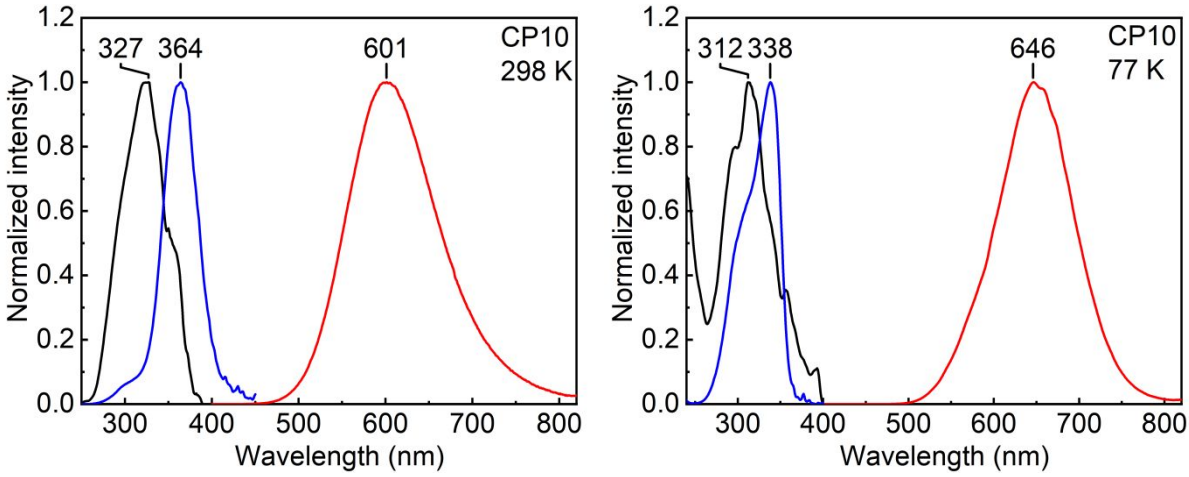

Figure S30. Solid-state absorption (black), emission (red) and excitation (blue) spectra for **CP10** at 298 K (left, λ_{ex} = 360 nm, λ_{em} = 600 nm) and 77 K (right, λ_{ex} =340 nm, λ_{em} = 640 nm).

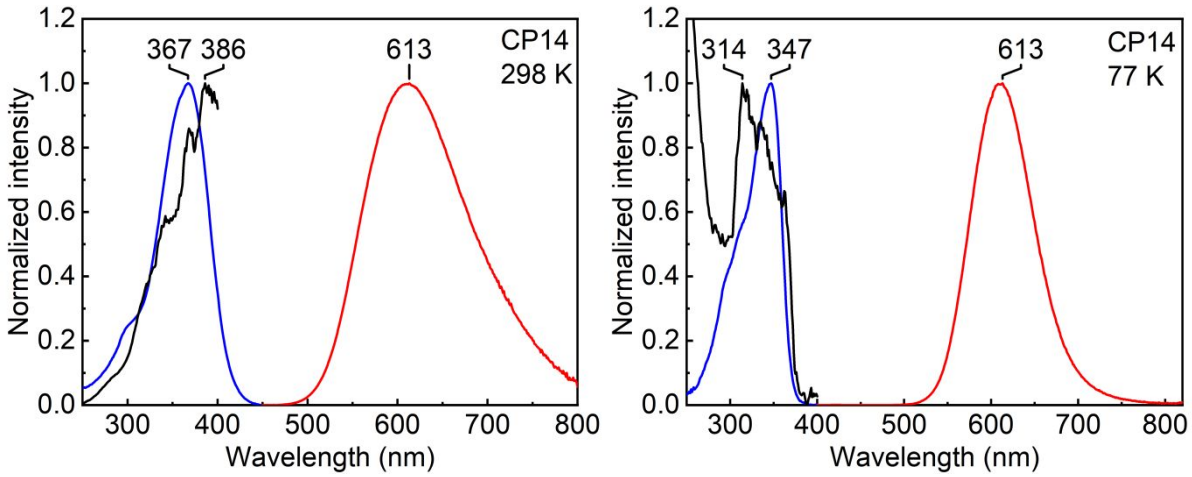

Figure S31. Solid-state absorption (black), emission (red) and excitation (blue) spectra for **CP14** at 298 K (left, λ_{ex} = 370 nm, λ_{em} = 610 nm) and 77 K (right, λ_{ex} =350 nm, λ_{em} = 610 nm).

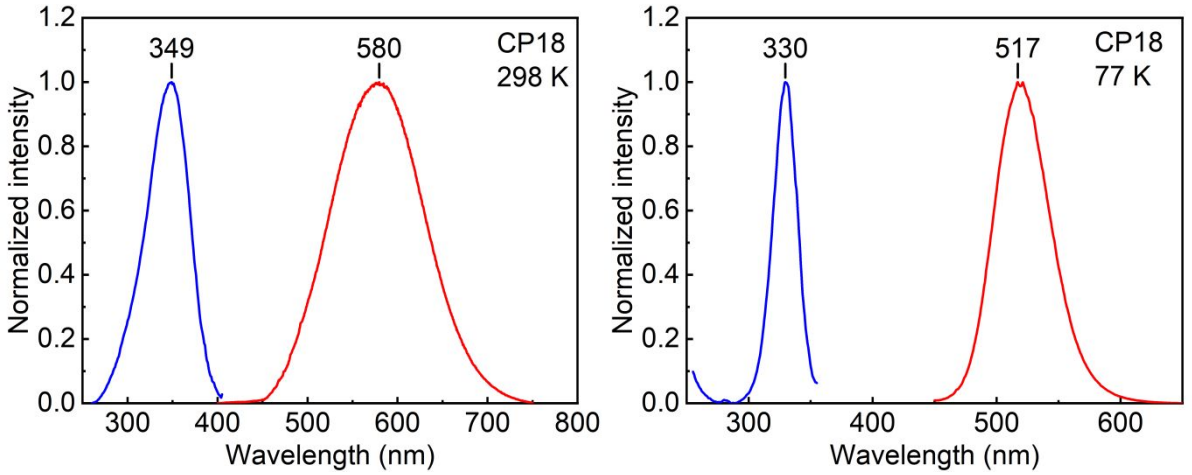

Figure S32. Solid state emission (red) and excitation (blue) spectra for **CP18** at 298 K (left, λ_{ex} = 350 nm, λ_{em} = 580 nm) and 77 K (right, λ_{ex} =330 nm, λ_{em} = 520 nm).

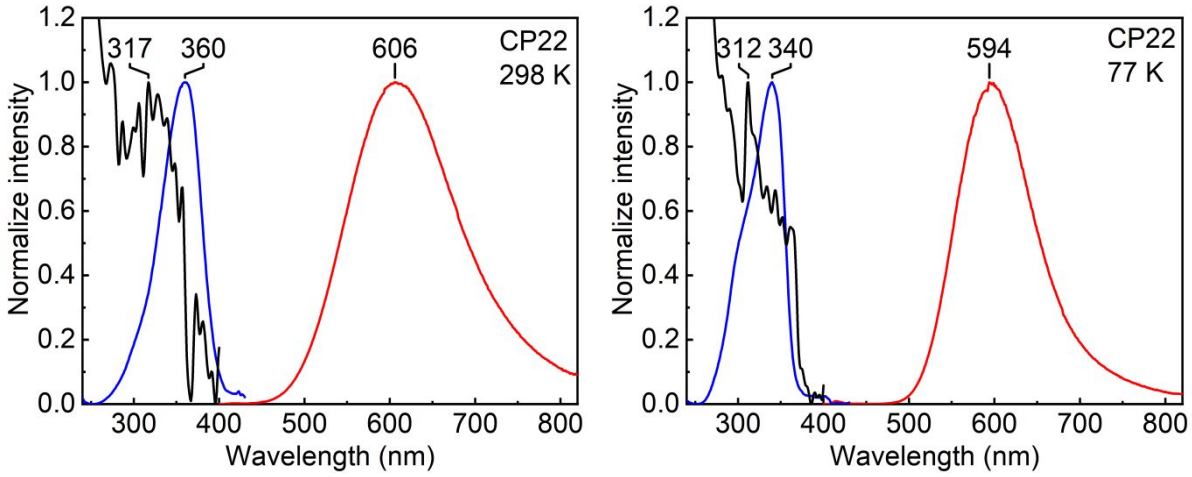

Figure S33. Solid-state absorption (black), emission (red) and excitation (blue) spectra for **CP22** at 298 K (left, λ_{ex} = 360 nm, λ_{em} = 600 nm) and 77 K (right, λ_{ex} =340 nm, λ_{em} = 590 nm).

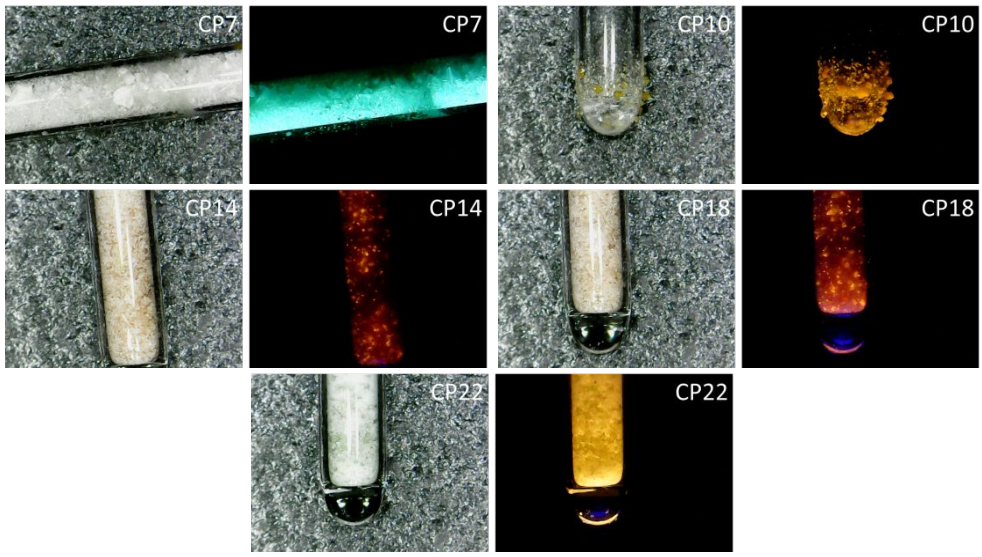

Figure S34. Crystalline sample of **CP7, CP10, CP14, CP18** and **CP22** inside glass capillary under white light and UV lamp (λ = 365 nm) irradiation.

Emission lifetimes

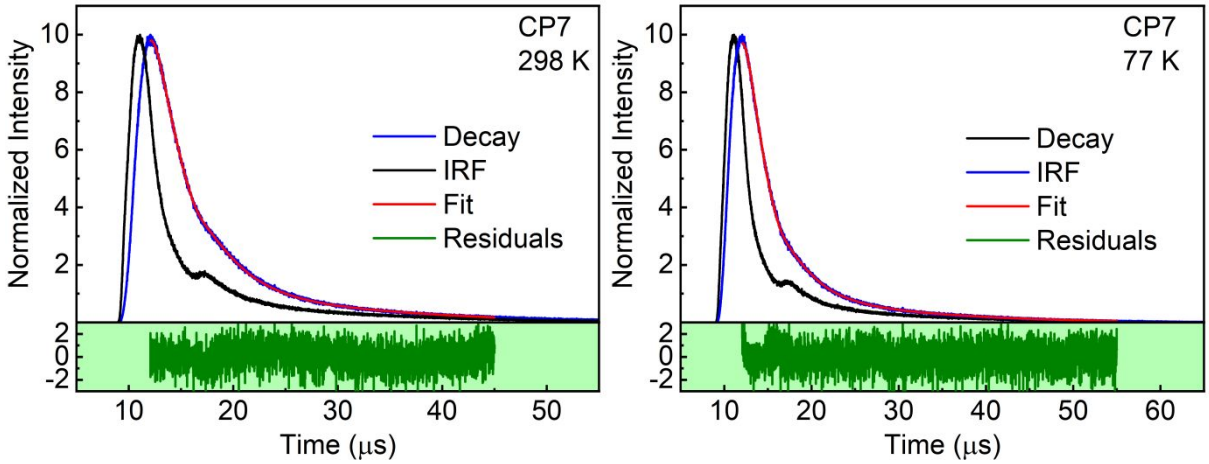

Figure S35. Decay of emission intensity (blue), fit (red), IRF (black) and residual (green) of **CP7**. Left, at 298 K, λ = 500 nm (λ_{ex} = 370 nm), τ_e {B}= 1.82 μs {0.0083}, χ^2 = 1.02. Right, at 77 K, λ = 500 nm (λ_{ex} = 350 nm), τ_e {B} = 2.13 μs {0.0073}, χ^2 = 1.00.

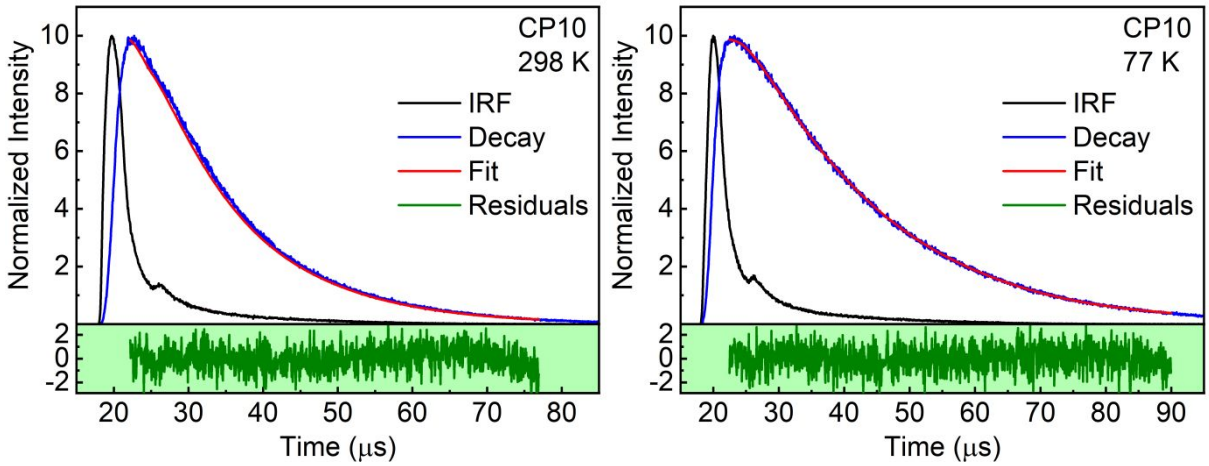

Figure S36. Decay of emission intensity (blue), fit (red), IRF (black) and residual (green) of **CP10**. Left, at 298 K, λ = 600 nm (λ_{ex} = 360 nm), τ_e {B}= 8.85 μs {0.0217}, χ^2 = 1.05. Right, at 77 K, λ = 640 nm (λ_{ex} = 340 nm), τ_e {B} = 14.94 μs {0.0191}, χ^2 = 1.02.

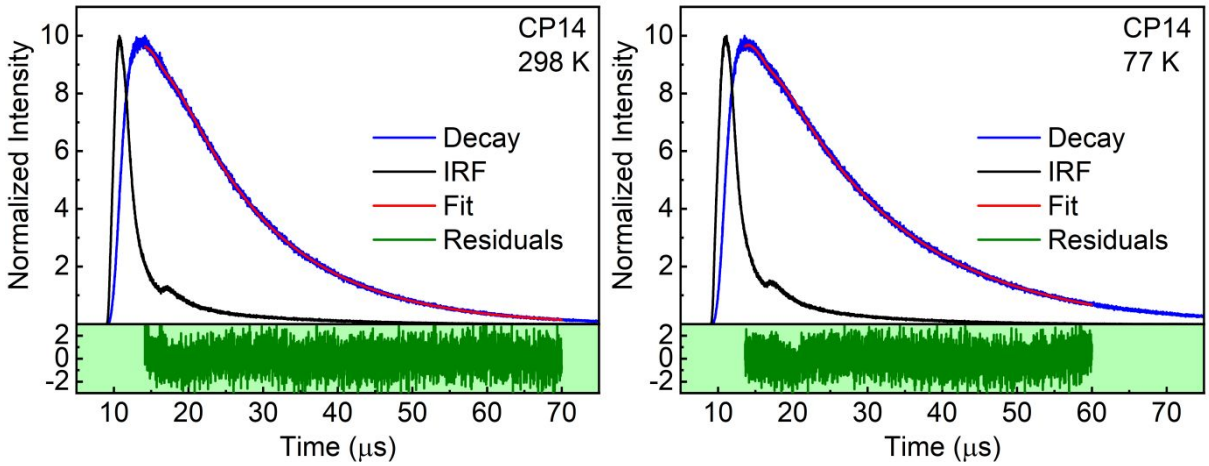

Figure S37. Decay of emission intensity (blue), fit (red), IRF (black) and residual (green) of **CP14**. Left, at 298 K, λ = 610 nm (λ_{ex} = 360 nm), τ_e {B}= 9.26 μs {0.0046}, χ^2 = 1.02. Right, at 77 K, λ = 610 nm (λ_{ex} = 350 nm), τ_e {B} = 8.12 μs {0.0050}, χ^2 = 1.03.

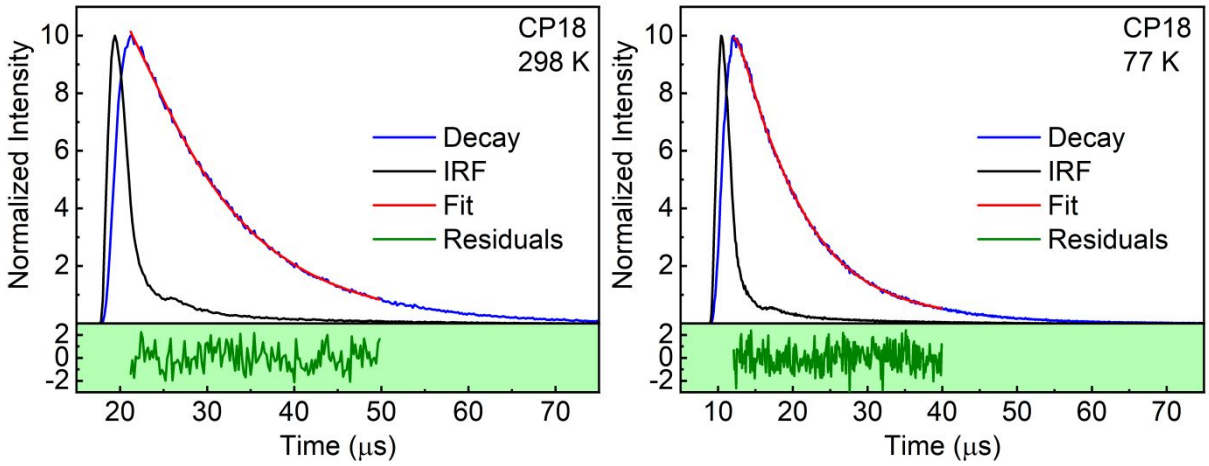

Figure S38. Decay of emission intensity (blue), fit (red), IRF (black) and residual (green) of **CP18**. Left, at 298 K, λ = 580 nm (λ_{ex} = 350 nm), τ_e {B}= 8.66 μs {0.1218}, χ^2 = 1.09. Right, at 77 K, λ = 520 nm (λ_{ex} = 330 nm), τ_e {B} = 6.34 μs {0.0622}, χ^2 = 1.04.

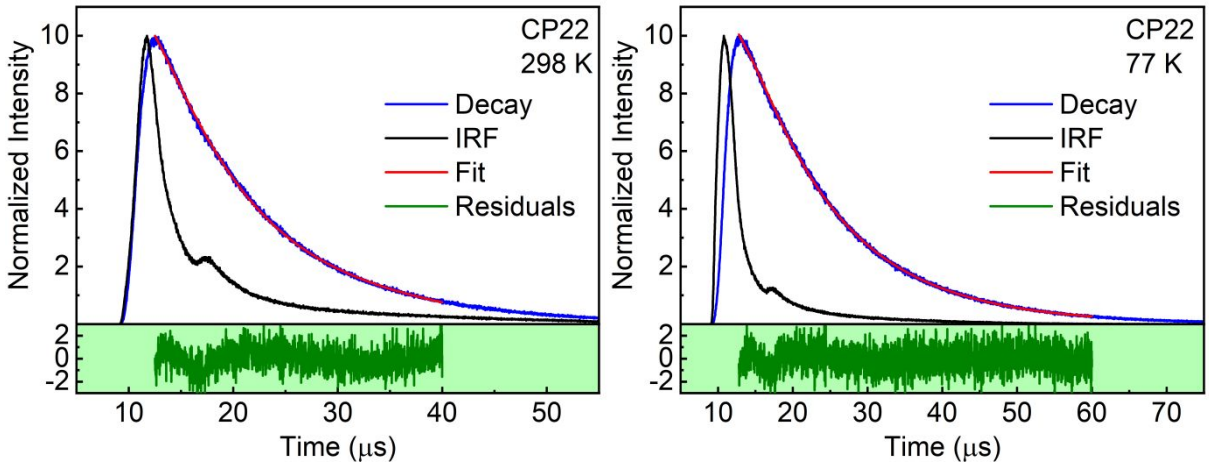

Figure S39. Decay of emission intensity (blue), fit (red), IRF (black) and residual (green) of **CP22**. Left, at 298 K, λ = 600 nm (λ_{ex} = 360 nm), τ_e {B}= 6.29 μs {0.0126}, χ^2 = 1.03. Right, at 77 K, λ = 590 nm (λ_{ex} = 340 nm), τ_e {B} = 8.57 μs {0.0106}, χ^2 = 1.05.

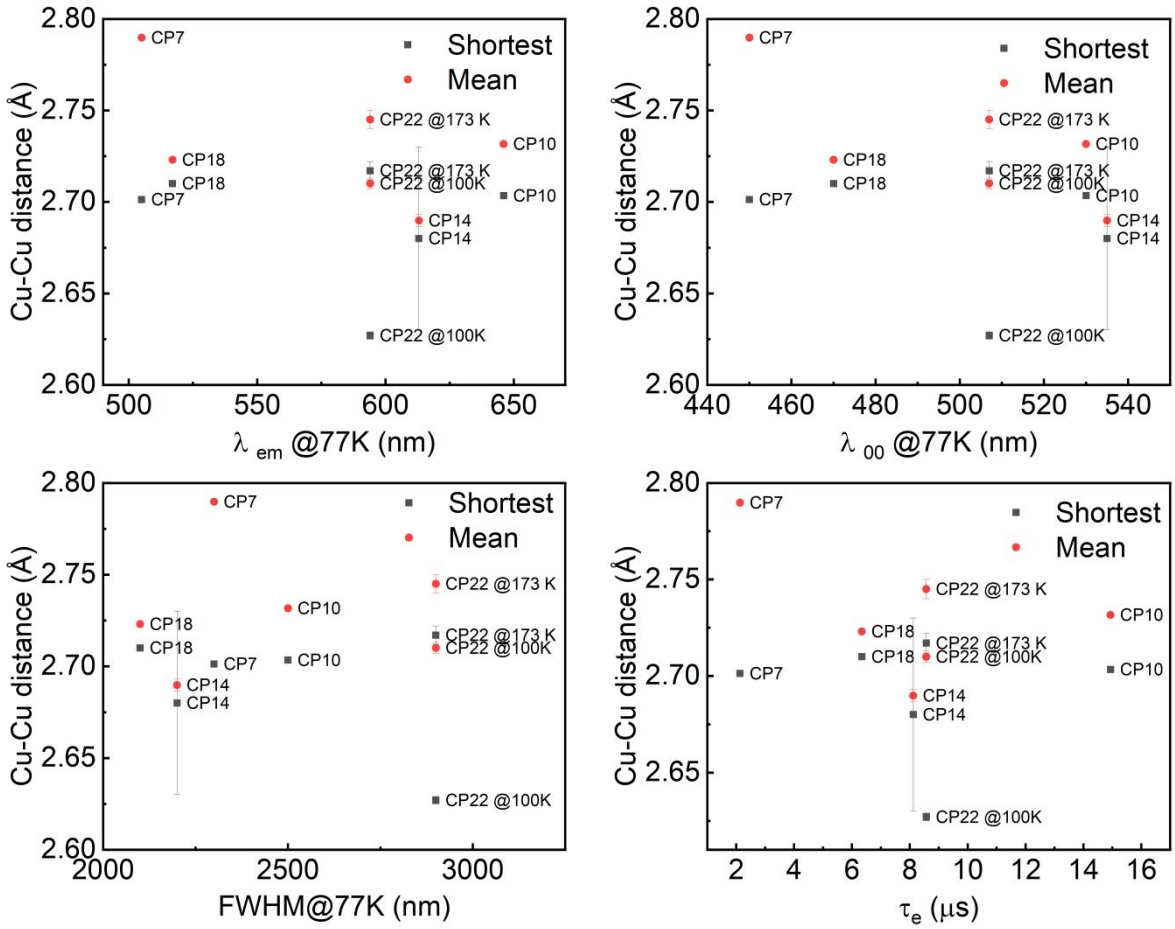

Figure S40. Shortest and mean Cu-Cu distances *vs* photophysical parameters of **CP4**, **CP8**, **CP11**, **CP15**, **CP19** and **CP23**. Error bars represent the standard uncertainty on bond length determined by X-ray diffraction.

Table S7. Photophysical data of thioether-containing cubanes and related species in 0D-3D

Ref.	Cluster	Dimensionality	*T* (K)	λ_{em} (nm) {fwhm} [Φ]	τ_p (μs)	Ligand
[7]	Cu_4I_4	2D	298 77	575 600	0.85 ± 0.01 3.36 ± 0.01	$PhS(CH_2)_4SPh$
[7]	Cu_6I_6	2D	298 77	555 565	2.62 ± 0.03 3.40 ± 0.06	$PhSCH_2C{\equiv}CCH_2SPh$
[8]	Cu_4I_4	1D	298 77	565 {3680} 565 {1900}	7.34 ± 0.05 8.80 ± 0.06	SEt_2
[9]	Cu_4I_4	2D	298 77	575 550	8.26 ± 0.18 5.96 ± 0.21	$nBuS(CH_2)_4SnBu$
[9]	Cu_4I_4	2D	298 77	547 540	4.69 ± 0.13 3.99 ± 0.56	$tBuS(CH_2)_4StBu$
[10]	Cu_4I_4	2D	298 77	520 525	1.64 ± 0.01 6.03 ± 0.10	$PhS(CH_2)_3SPh$
[10]	Cu_4I_4	1D	298 77	560 555	1.04 ± 0.05 8.04 ± 0.01	$PhS(CH_2)_5SPh$
[11]	Cu_4I_4	?	298 77	560 560	7.00 ± 0.50 7.20 ± 0.01	$CyS(CH_2)_4SCy$
[12]	Cu_4I_4	2D	298 77	520 520	1.24 ± 0.02 4.46 ± 0.01	$pTolSCH_2C{\equiv}CCH_2SpTol$
[6]	Cu_4I_4	1D	298 77	515 515	1.0 ± 0.1 1.2 ± 0.1	$PhSCH_2SPh$
[6]	Cu_4I_4	1D	298 77	500 510	1.4 ± 0.1 1.4 ± 0.1	$pTolSCH_2SpTol$
[6]	Cu_4I_4	1D	298 77	550 546	10.3 ± 0.1 4.2 ± 0.2	$MeOPhSCH_2SPhOMe$
[6]	Cu_4I_4	1D	298 77	537 520	10.3 ± 0.1 5.9 ± 0.1	$mTolo^tBuSCH_2SmTolo^tBu$
[6]	Cu_4I_4	1D	298 77	570 690	1.1 ± 0.1 9.2 ± 0.1	$mTolSCH_2SmTol$
[5]	Cu_4I_4	1D	298 77	525 {3600} 530 {2580}	4.02 ± 0.01 4.18 ± 0.01	$PhS(CH_2)_8SPh$
[5]	Cu_8I_8	2D	298 77	525 {2580} 538 {1820}	2.72 ± 0.01 5.27 ± 0.01	$pTolS(CH_2)_8SpTol$
13	Cu_4I_4	2D	298 77	549 551	5.04 ± 0.09 15.71 ± 0.23	MeSMe
13	Cu_4I_4	1D	298 77	550 540	4.66 ± 0.04 11.55 ± 0.25	MeSEt
13	Cu_4I_4	1D	298 77	544 535	6.74 ± 0.25 8.49 ± 0.09	MeSPr
13	Cu_4I_4	0D	298 77	623 667	2.57 / 5.17 ± 0.01 1.93 / 2.08 ± 0.01	EtSPr
13	Cu_4I_4	0D	298 77	618 601	3.57 / 12.75 1.02 / 3.51	PrSPr
13	Cu_4I_4	0D	298 77	526 503	0.45 2.12	$iPrSiPr$
13	Cu_8I_8	0D	298 77	573 [0.45] 542	0.20 0.26 / 2.69 ± 0.01	$iPrSiPr$
14	Cu_4I_4	2D	298 77	515 569	1.03 ± 0.11 1.32 ± 0.01	$PhSCH_2C{=}CCH_2SPr$ (cis)
15	Cu_4I_4	1D	298 77	533 [0.21] -	2.81 -	$tBuS(CH_2)_8StBu$
15	Cu_8I_8	2D	298 77	561 [0.40] -	5.11 -	$pTolS(CH_2)_8SpTol$
16	Cu_4I_4	2D	298 77	585 588	8.94 ± 0.30 8.36 ± 0.30	EtSEt
17	Cu_8I_8 (open)	3D	298 77	534 {5900} [0.36] 574 {2900}	2.41 2.51	2-Methyl-1,3-dithiane

References

(1) Dolomanov, O. V.; Bourhis, L. J.; Gildea, R. J.; Howard, J. A. K.; Puschmann, H. OLEX2 : A Complete Structure Solution, Refinement and Analysis Program. *J. Appl. Crystallogr.* **2009**, *42* (2), 339–341. https://doi.org/10.1107/S0021889808042726.

(2) Sheldrick, G. M. A Short History of SHELX. *Acta Crystallogr. Sect. A Found. Crystallogr.* **2008**, *64* (1), 112–122. https://doi.org/10.1107/S0108767307043930.

(3) Sheldrick, G. M. Crystal Structure Refinement with SHELXL. *Acta Crystallogr. Sect. C Struct. Chem.* **2015**, *71* (1), 3–8. https://doi.org/10.1107/S2053229614024218.

(4) Hartley, F. R.; Murray, S. G.; Levason, W.; Soutter, H. E.; McAuliffe, C. A. Systematics of Palladium(II) and Platinum(II) Dithioether Complexes. The Effect of Ligand Structure upon the Structure and Spectra of the Complexes and upon Inversion at Coordinated Sulphur. *Inorganica Chim. Acta* **1979**, *35* (C), 265–277. https://doi.org/10.1016/S0020-1693(00)93450-9.

(5) Harvey, P. D.; Bonnot, A.; Lapprand, A.; Strohmann, C.; Knorr, M. Coordination RC6H4S(CH2)8SC6H4R/(CuI)n Polymers (R (n) = H(4); Me (8)): An Innocent Methyl Group That Makes the Difference. *Macromol. Rapid Commun.* **2015**, *36* (7), 654–659. https://doi.org/10.1002/marc.201400659.

(6) Knorr, M.; Khatyr, A.; Dini Aleo, A.; El Yaagoubi, A.; Strohmann, C.; Kubicki, M. M.; Rousselin, Y.; Aly, S. M.; Fortin, D.; Lapprand, A.; et al. Copper(I) Halides (X = Br, I) Coordinated to Bis(Arylthio)Methane Ligands: Aryl Substitution and Halide Effects on the Dimensionality, Cluster Size, and Luminescence Properties of the Coordination Polymers. *Cryst. Growth Des.* **2014**, *14* (11), 5373–5387. https://doi.org/10.1021/cg500905z.

(7) Knorr, M.; Guyon, F.; Khatyr, A.; Däschlein, C.; Strohmann, C.; Aly, S. M.; Abd-El-Aziz, A. S.; Fortin, D.; Harvey, P. D. Rigidity effect of the dithioether spacer on the size of the luminescent cluster (Cu2I2)n (n = 2, 3) in their coordination polymers. *J. Chem. Soc. Dalt. Trans.* **2009**, *0* (6), 948–955. https://doi.org/10.1039/b816987j.

(8) Knorr, M.; Pam, A.; Khatyr, A.; Strohmann, C.; Kubicki, M. M.; Rousselin, Y.; Aly, S. M.; Fortin, D.; Harvey, P. D. Reactivity of CuI and CuBr toward Et2S: A Reinvestigation on the Self-Assembly of Luminescent Copper(I) Coordination Polymers. *Inorg. Chem.* **2010**, *49* (13), 5834–5844. https://doi.org/10.1021/ic901906h.

(9) Knorr, M.; Guyon, F.; Kubicki, M. M.; Rousselin, Y.; Aly, S. M.; Harvey, P. D. Effect of t-BuS vs. n-BuS on the topology, Cu···Cu distances and luminescence properties of 2D Cu4I4/RS(CH2)4SR metal-organic frameworks. *New J. Chem.* **2011**, *35* (6), 1184–1188. https://doi.org/10.1039/c0nj00923g.

(10) Knorr, M.; Guyon, F.; Khatyr, A.; Strohmann, C.; Allain, M.; Aly, S. M.; Lapprand, A.; Fortin, D.; Harvey, P. D. Construction of (CuX)2n Cluster-Containing (X = Br, I; n = 1, 2) Coordination Polymers Assembled by Dithioethers ArS(CH 2) m SAr (Ar = Ph, p -Tol; m = 3, 5): Effect of the Spacer Length, Aryl Group, and Metal-to-Ligand Ratio on the Dimensionality, Clus. *Inorg. Chem.* **2012**, *51*, 9917–9934. https://doi.org/10.1021/ic301385u.

(11) Bonnot, A.; Strohmann, C.; Knorr, M.; Harvey, P. D. Metal-to-Ligand Ratio Effect on the Size of Copper Iodide and Copper Bromide Clusters in 1,4-Bis(Cyclohexylthio)Butane-Spanned Coordination Polymers. *J. Clust. Sci.* **2014**, *25* (1), 261–275. https://doi.org/10.1007/s10876-013-0637-5.

(12) Bonnot, A.; Knorr, M.; Strohmann, C.; Golz, C.; Fortin, D.; Harvey, P. D. CuX (X = Cl, Br, I) Containing Coordination Polymers Built Upon Isomeric RSCH2C≡CCH2SR (R = p-Tolyl, Benzyl) Dithioether Ligands: First Example of a Luminescent (CuCl)n/Dithioether Network. *J. Inorg. Organomet. Polym. Mater.* **2015**, *25* (3), 480–494. https://doi.org/10.1007/s10904-015-0204-7.

(13) Knorr, M.; Bonnot, A.; Lapprand, A.; Khatyr, A.; Strohmann, C.; Kubicki, M. M.; Rousselin, Y.; Harvey, P. D. Reactivity of CuI and CuBr toward Dialkyl Sulfides RSR: From Discrete

Molecular Cu4I4S4 and Cu8I8S6 Clusters to Luminescent Copper(I) Coordination Polymers. *Inorg. Chem.* **2015**, *54* (8), 4076–4093. https://doi.org/10.1021/acs.inorgchem.5b00327.

(14) Bonnot, A.; Knorr, M.; Guyon, F.; Kubicki, M. M.; Rousselin, Y.; Strohmann, C.; Fortin, D.; Harvey, P. D. 1,4-Bis(Arylthio)but-2-Enes as Assembling Ligands for (Cu2X2)n (X = I, Br; N = 1, 2) Coordination Polymers: Aryl Substitution, Olefin Configuration, and Halide Effects on the Dimensionality, Cluster Size, and Luminescence Properties. *Cryst. Growth Des.* **2016**, *16* (2), 774–788. https://doi.org/10.1021/acs.cgd.5b01360.

(15) Bonnot, A.; Juvenal, F.; Lapprand, A.; Fortin, D.; Knorr, M.; Harvey, P. D. Can a Highly Flexible Copper(i) Cluster-Containing 1D and 2D Coordination Polymers Exhibit MOF-like Properties? *Dalt. Trans.* **2016**, *45*, 11413–11421. https://doi.org/10.1039/c6dt01375a.

(16) Bonnot, A.; Karsenti, P.-L.; Juvenal, F.; Golz, C.; Strohmann, C.; Fortin, D.; Knorr, M.; Harvey, P. D. The 3D [(Cu2Br2){μ-EtS(CH2)4SEt}]n Material: A Rare Example of a Coordination Polymer Exhibiting Triplet–Triplet Annihilation. *Phys. Chem. Chem. Phys.* **2016**, *18* (36), 24845–24849. https://doi.org/10.1039/C6CP04728A.

(17) Schlachter, A.; Viau, L.; Fortin, D.; Knauer, L.; Strohmann, C.; Knorr, M.; Harvey, P. D. Control of Structures and Emission Properties of (CuI)n 2-Methyldithiane Coordination Polymers. *Inorg. Chem.* **2018**, *57*, 13564–13576. https://doi.org/10.1021/acs.inorgchem.8b02168.